Accepted Manuscript

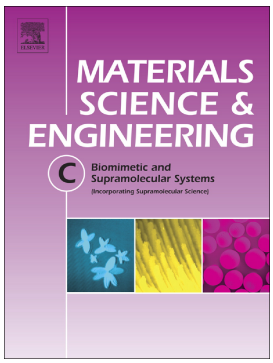

Direct electrochemistry of glucose oxidase based on one step electrodeposition of reduced graphene oxide incorporating polymerized l-lysine and its application in glucose sensing

Dongdong Zhang, Xia Chen, Weina Ma, Tianfeng Yang, Dandan Li, Bingling Dai, Yanmin Zhang

PII: S0928-4931(17)34856-7
DOI: https://doi.org/10.1016/j.msec.2019.109880
Article Number: 109880
Reference: MSC 109880

To appear in: *Materials Science & Engineering C*

Received date: 15 December 2017
Revised date: 22 January 2019
Accepted date: 10 June 2019

Please cite this article as: D. Zhang, X. Chen, W. Ma, et al., Direct electrochemistry of glucose oxidase based on one step electrodeposition of reduced graphene oxide incorporating polymerized l-lysine and its application in glucose sensing, Materials Science & Engineering C, https://doi.org/10.1016/j.msec.2019.109880

Direct electrochemistry of glucose oxidase based on one step electrodeposition of reduced graphene oxide incorporating polymerized L-lysine and its application in glucose sensing

Dongdong Zhang, Xia Chen, Weina Ma, Tianfeng Yang, Dandan Li, Bingling Dai, Yanmin Zhang*

School of Pharmacy, Xi'an Jiaotong University, Xi'an 710061, China

*Corresponding author. Tel: +86 02982656264, Fax: +86 02982655451

Email address: zhang2008@mail.xjtu.edu.cn

ABSTRACT

The direct electron transfer and enzyme catalytic activity were investigated in electrochemical biosensor based on glucose oxidase (GOx) and electrochemical reduced graphene oxide-poly-(L-lysine) (ERGO-PLL) hybrid composite film embedded in a biocompatible matrix of Nafion. The ERGO-PLL was fabricated onto glassy carbon electrode (GCE) through one step electrodeposition of RGO incorporating PLL from graphene oxide-L-lysine aqueous dispersion. The fabrication process of Nafion/GOx/ERGO-PLL/GCE has been characterized by cyclic voltammetry and electrochemical impedance spectroscopy, and the surface morphology of modified electrodes were characterized by scanning electron microscopy. A pair of well-defined redox peaks with formal potential and peak separation of -0.461 V and 30 mV were observed at scan rate of 50 mV s^{-1}, the electron transfer rate constant was calculated to be 18.7 s^{-1}, demonstrated that direct electron transfer between immobilized GOx with ERGO-PLL and GCE was achieved. Moreover, the fabricated enzyme biosensor exhibited excellent electrocatalytic activity for determination of glucose in O_2-free PBS (7.40) with linear voltammetric response from 0.005 to 9.0 mmol L^{-1}, and detection limits (S/N=3) of 2.0 μmol L^{-1}. This work indicates that ERGO-PLL based modified electrode is superior to that of graphene based, and could be applied in biosensors, bioelectronics and electrocatalysis, etc.

Keywords: Glucose oxidase; Graphene; L-lysine; Electron transfer; Electrochemical biosensor

1. Introduction

Direct electron transfer (DET) between the cofactor of a redox active enzyme (oxidoreductase) or a redox protein and an electrode is significant to the development of electrochemical devices for sensing and energy conversion [1]. DET is rarely observed and reported for only few redox enzymes/proteins and it is seldom detected between these enzymes/proteins and a bare electrode in the absence of redox mediators. Mostly, this is due to the fact that the redox active centers of the enzymes/proteins are deeply buried in their surrounding globular protein structures. A number of studies have been carried out to facilitate electron transfer between the redox active site of the enzymes/proteins and electrode [2, 3]. Various nanomaterials such as carbon nanotubes[4], carbon ionic liquid [5], graphite nanoparticles [6], graphene nanosheets [7] and other nanocomposites, etc. [8] have been employed to achieve DET by decreasing long electron-tunneling distance.

Glucose oxidase (GOx) is an oxidoreductase which consists of two identical polypeptide chains containing a redox center (FAD and $FADH_2$), it catalyses the oxidation of glucose to gluconolactone with the consumption of oxygen and production of hydrogen peroxide [9]. Achieving the direct electron transfer of GOx depends significantly on the distance between the redox center and the electrode surface. Graphene, a two-dimensional (2D) planar structure of sp^2 carbon atoms, has attracted considerable attention in recent years, especially been used for construction of electrochemical biosensors applications [10, 11]. Numerous studies report successful achievements of the direct electron transfer of GOx based on graphene [7, 12]. Furthermore, graphene-based hybrids composites including graphene/AuNPs/chitosan nanocomposite film [13], graphene-conducting polyaniline composite [14], graphene-polyethyleneimine-AuNPs hybrid [15], ZnO-nanorods/graphene heterostructure [16],

triethylenetetramine-functionalized graphene [17] and reduced graphene oxide-magnetic nanoparticles nanocomposite [18] have been employed to achieve DET of GOx and further to apply in glucose sensitive determination.

Lysine, an α-amino acid, is used in the biosynthesis of proteins. It contains an α-amino group that is in the protonated $-NH_3^+$ form under physiological conditions. Electropolymerization is effective method for electrode modification action with a property of desired matrices, homogeneity in electrochemical deposition, good stability and strong adherence to electrode surface [19]. Poly-L-lysine (PLL) has been employed as a conductive polymer in the construction of electrochemical sensors for dissolved oxygen [20], glucose [21] and protein [22], etc. because of its simple and rapid preparation, good biocompatibility and reproducibility. Electropolymerized PLL is used as a positively charged polymer interface to adsorb GO nanosheets, and then adsorbed GO was electrochemically reduced by cyclic voltammetry to prepare ERGO/PLL/GCE [21]. Our previous work developed the preparation method with directly electrodeposited reduced graphene oxide from GO dispersions based on electropolymerized PLL of positively charged polymer as an electrode interface to adsorb negatively charged GO nanosheets by electrostatic attraction [23].

This study reported a novel method to construct an ERGO-PLL hybrid composite onto GCE through one step electrodeposition of reduced graphene oxide incorporating polymerized L-lysine from graphene oxide-L-lysine aqueous dispersion. The thickness of functionalized graphene film can be easily controlled by using the electrodeposition technique, a distinct advantage over previously developed methods. The direct electron transfer and enzyme catalytic activity were investigated in electrochemical biosensor based on GOx and ERGO-PLL hybrid composite film embedded in a biocompatible matrix of Nafion. The fabrication process of

Nafion/GOx/ERGO-PLL/GCE was analyzed with cyclic voltammetry and electrochemical impedance spectroscopy, and the surface morphology of the modified electrodes were characterized by scanning electron microscopy (SEM). The electrochemical properties and electrocatalytic activities toward glucose of the modified electrodes were demonstrated.

2. Experimental

2.1. Reagents and apparatus

Graphene oxide was prepared by the Hummers method [24, 25]. The prepared GO was dispersed in 10 mM sodium phosphate buffer saline (PBS, pH 7.40) to get the 1.0 mg mL^{-1} suspension. Glucose, Glucose Oxidase (GOx, 140 U mg^{-1}), L-lysine and Nafion perfluorinated resin solution (5 wt.% in lower aliphatic alcohols and water, contains 15% water) were obtained from Sigma-Aldrich. Other reagents are analytical grade. Millipore Milli-Q water (18 MΩ cm) is used in all experiments.

Fourier transform infrared (FT-IR) measurements were performed with a System 2000 infrared spectrometer (Perkin Elmer, America) with a KBr plate. Images of SEM were captured using TM-1000 tabletop microscope (Hitachi, Japan). All electrochemical measurements were determined on CHI 660D electrochemical workstation (Shanghai Chenhua, China) using a conventional three-electrode system, where a GCE (diameter 3.0 mm) was used as the working electrode, a platinum wire counter electrode, and a saturated Ag/AgCl electrode reference electrode. All voltammetric measurements were performed from negative potential to positive potential, and before all voltammetric measurements (unless otherwise noted), sample solutions were purged with nitrogen for at least 20 min to remove oxygen. The parameters applied for the square wave voltammetry were as follows: 25 mV, 15 Hz and 2.0 s were chosen for amplitude, frequency and quiet time, respectively. 10 mM

PBS (pH 7.40) containing 100 mM KCl was used as electrolyte.

2.2. Preparation of modified electrodes

GCE was firstly polished using 0.3, 0.1 and 0.05 μm alumina slurry followed by rinsing thoroughly with water. Then, the clean GCE was performed with one step electrodeposition of reduced graphene oxide incorporating polymerized L-lysine from -1.5 V to 2.2 V for 8 circles at a scan rate of 25 mV s^{-1}, in a N_2-saturated 100 mM KCl-10 mM PBS (pH 7.40) containing 1.0 mg mL^{-1} GO and 1.0 mM L-lysine (5:2, v/v) aqueous dispersion, under a continuously stirring condition. After that, 5 μL Glucose Oxidase of 5 mg mL^{-1} was dropped onto the effective surface of ERGO-PLL/GCE, dried in 4 ºC refrigerator for 2 hours. Subsequently, 4 μL Nafion of 0.5 wt.% diluted with ethanol (⩾99.7) was dropped onto the modified electrode which was constructed a thin film to prevent the leakage of adsorbed GOx (denoted as Nafion/GOx/ERGO-PLL/GCE). For comparison, PLL/GCE and ERGO/GCE were prepared using GCE in the N_2-saturated 100 mM KCl-10 mM PBS (pH 7.40) containing either 1.0 mM L-lysine or 1.0 mg mL^{-1} GO aqueous solution with the same electrodeposition conditions as that for the ERGO-PLL/GCE. Nafion/GOx/GCE, Nafion/GOx/PLL/GCE and Nafion/GOx/ERGO/GCE were prepared using GCE, PLL/GCE and ERGO/GCE with the same modified process as that for the Nafion/GOx/ERGO-PLL/GCE, respectively. All modified electrodes obtained were rinsed with water thoroughly and were stored at 4 °C when not in use.

3. Results and discussion

3.1. FT-IR spectroscopic characterization of GO with L-lysine

Fig. 1 displays FT-IR spectra of GO, L-lysine and GO-L-Lys. The FT-IR spectrum of GO (curve, a) shows that a broad and intense peak of O-H group at 3140 cm^{-1}, a C=O peak at 1643 cm^{-1}, a C-OH stretching peak at 1134 cm^{-1}. These

confirmed a successful oxidation of graphite, and there were a number of hydrophilic groups, i.e., -OH, -COOH and epoxides in the surface of GO obtained [26]. The FT-IR spectrum of L-lysine (curve, b) shows a peak 1597 cm^{-1} originating from the carboxyl double bond, the 1512 cm^{-1} peak and 1340 cm^{-1} peak are indicative of an NH bending and the NH_2 vibration, respectively. And the 1404 cm^{-1} peak is indicative of free lysine [27]. The adsorption of L-lysine onto the GO leads to a shift of the vibration at 1597 cm^{-1} and 1512 cm^{-1} to 1659 cm^{-1} and 1520 cm^{-1} respectively. While the vibration at 1404 is unchanged (curve, c). This is maybe attributed to that the impact of electrostatic interaction between the negatively charged GO nanosheets and positively charged L-lysine, suggesting that L-lysine is successfully bound to the GO nanosheets.

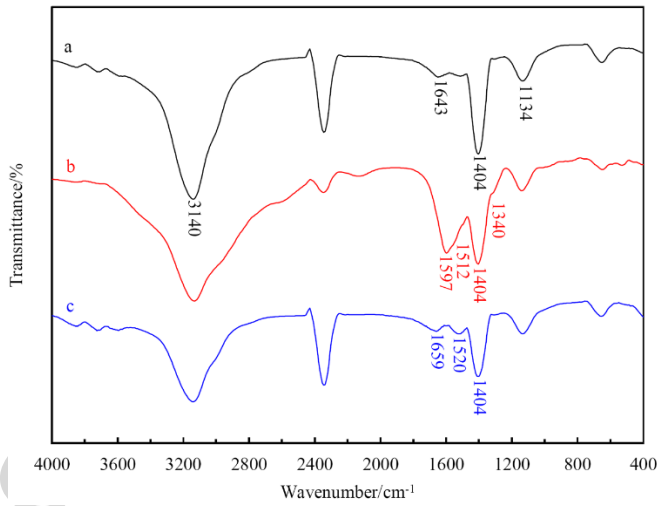

Figure 1 FT-IR spectra of graphene oxide (curve a), L-lysine (curve b) and graphene oxide-L-lysine (curve c).

3.2. Preparation and electrochemical characterization of ERGO-PLL/GCE

As shown in Fig. 2, for the amplified part of the first voltammetric cycle in the inset, it can be seen that an oxidation onset potential of bare GCE appears at about +1.2 V and a reduction peak appears at -0.6 V. This might attributed to that the electrode activation process of a freshly polished GCE, which introduced some

oxygen-containing functional groups including phenolic and carbonyl groups, as well as evolved oxygen was derived from oxidation of water, could be created on the surface of GCE [28]. From the second voltammetric cycle, the oxidation onset potential appears at about +0.8 V and an oxidation peak occurs at about +1.3 V, which might ascribed to that the oxidation process of L-lysine. And a wider reduction peak appears at approximately from -0.4 V to -0.8 V, which might ascribed to that the merged reduction process of L-lysine and actively evolved oxygen. In addition, the cyclic voltammograms exhibits the other oxidation peak around 0 V from the second cycle, which could be assigned to the incorporation of quinone groups at the activated GCE electrode surface [28], as well as some oxygen-bearing groups of the electrodeposited ERGO [23]. Furthermore, it can further find that the redox peak currents and background currents rapidly increased and then negligibly changed from 3rd to 8th cycles. The increased currents could be assigned to the oxidation of L-lysine and the reduction of GO on the GCE surface, and the gradually growth of ERGO-PLL composite film along with the continuous electrode activation. In this work, 8 cycles were used for ERGO-PLL electrodeposition.

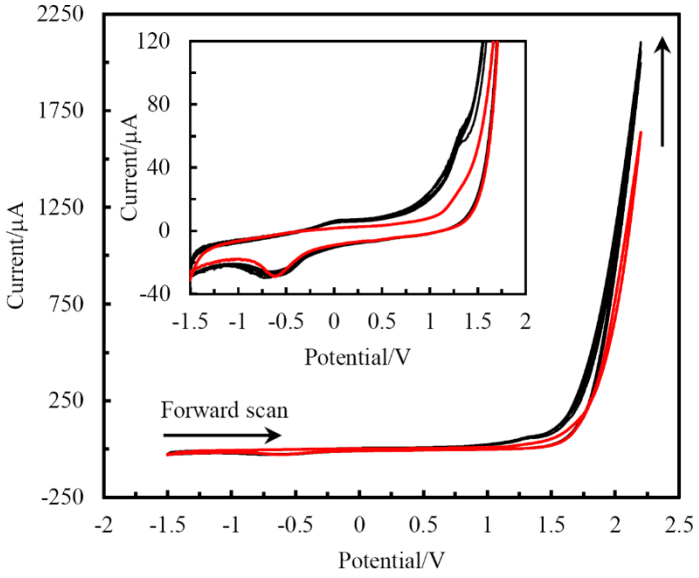

Figure 2 Cyclic voltammograms obtained of GCE in continuously stirring condition of

N_2-saturated 100 mM KCl-10 mM PBS (pH 7.40) containing 1.0 mg mL^{-1} GO and 1.0 mM L-lysine (5:2, v/v) scan from -1.5 V to 2.2 V for 8 circles with a scan rate of 25 mV s^{-1}.

3.3. Morphologic characterization of modified electrodes

From Fig. 3, it can be seen that the PLL nanoparticles were obtained on the surface of PLL/GCE (Fig. 3A), while the ERGO film exhibited a thin wrinkled paper like structure on the surface of ERGO/GCE (Fig. 3B). And the ERGO-PLL/GCE displayed not only ERGO film morphology but also PLL nanoparticles and homogeneously distributed on the GCE surface (Fig. 3C), which similar to that fabricated by firstly polymerized of L-lysine and electrodeposited reduced graphene oxide onto the GCE [23]. Furthermore, the PLL nanoparticles was distributed into the multi-layered structure of graphene nanosheets, leads to that the ERGO-PLL hybrid composite obtained with a similar three-dimensional structure. This is obviously beneficial to the subsequent GOx immobilization. The characterization demonstrates that the ERGO-PLL composite is successfully constructed on the GCE surface by proposed with here one step electrodeposition method. When the GOx enzyme was immobilized and then the Nafion film was covered on the surface of ERGO-PLL modified electrode, the Nafion/GOx/ERGO-PLL/GCE showed deposition of enzyme globular structure and nafion porous structure, indicating that the enzymes were successfully immobilized on the modified electrode surface (Fig. 3D).

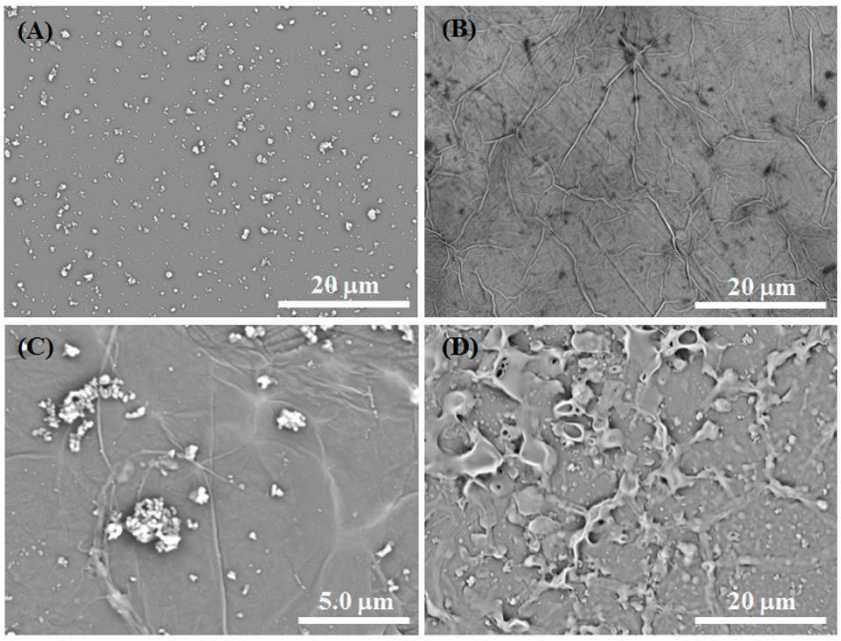

Figure 3 SEM images of PLL/GCE (A), ERGO/GCE (B), ERGO-PLL/GCE (C) and Nafion/GOx/ERGO-PLL/GCE (D).

3.4. Electrochemical characterization of modified electrodes

In order to monitor each immobilization step, corresponding cyclic voltammograms and impedance spectra in electroactive probes system of potassium ferricyanide and potassium ferrocyanide were recorded. Fig. 4A shows that a pair of redox peaks at bare GCE (curve, a) with a peak potential separation (ΔE_p) of 78 mV and the ratio of redox peak currents (i_{pa}/i_{pc}) is close to 1.0. While at ERGO-PLL/GCE (curve, b), the redox peak currents slightly increase (the increase rates for i_{pa} and i_{pc} are 12.4% and 13.7%, respectively.) and the value of ΔE_p changes to 68 mV. This could be ascribed to ERGO-PLL nanocomposite modified provides a large effective electrode surface area and with synergistic effects between ERGO and PLL [23]. For comparison at GOx/ERGO-PLL/GCE (curve, c), the redox peak currents clearly decrease (the rate of decrease for i_{pa} and i_{pc} were 52.9% and 46.7%, respectively.) and the value of ΔE_p clearly changes to 163 mV. This is probably attributed to the fact that an insulating layer of the immobilized GOx on the surface of ERGO-PLL composite

can hinder the electron transfer. While at Nafion/GOx/ERGO-PLL/GCE (curve, d), the redox peak currents further decrease (the decrease rates for i_{pa} and i_{pc} are 88.6% and 86.0%, respectively.) and the value of ΔE_p is slightly changes to 189 mV. This is attributed to the fact that covered Nafion film with negative charge can further hinder the electron transference of the $[Fe(CN)_6]^{3-/4-}$ probes to the electrode surface. These results indicate that the GOx modified electrode was successfully obtained.

Fig. 4B shows the EIS diagrams of the bare and modified GCEs. The R_{et} (34 Ω, curve b) of the ERGO-PLL/GCE was lower than that of the bare GCE (200 Ω, curve a), suggesting that ERGO-PLL composite film has been formed on the GCE surface, greatly improves the conductivity and the electron transfer process. When GOx was adsorbed into the ERGO-PLL film, the R_{et} increased distinctly to 1938 Ω (curve c), suggesting that the GOx was steadily adsorbed into the ERGO-PLL film, and hinder the electron transfer from the redox probe of $[Fe(CN)_6]^{3-/4-}$ to the electrode surface. When nafion was covered onto the GOx/ERGO-PLL modified layer, the R_{et} further increased to 5798 Ω (curve d), suggesting that a layer of nafion was formed, and with a little inhibition of the electron transfer of the redox couple. These results obtained from EIS are in agreement with the results obtained from cyclic voltammograms which demonstrated again that the proposed enzyme modified electrode was successfully fabricated.

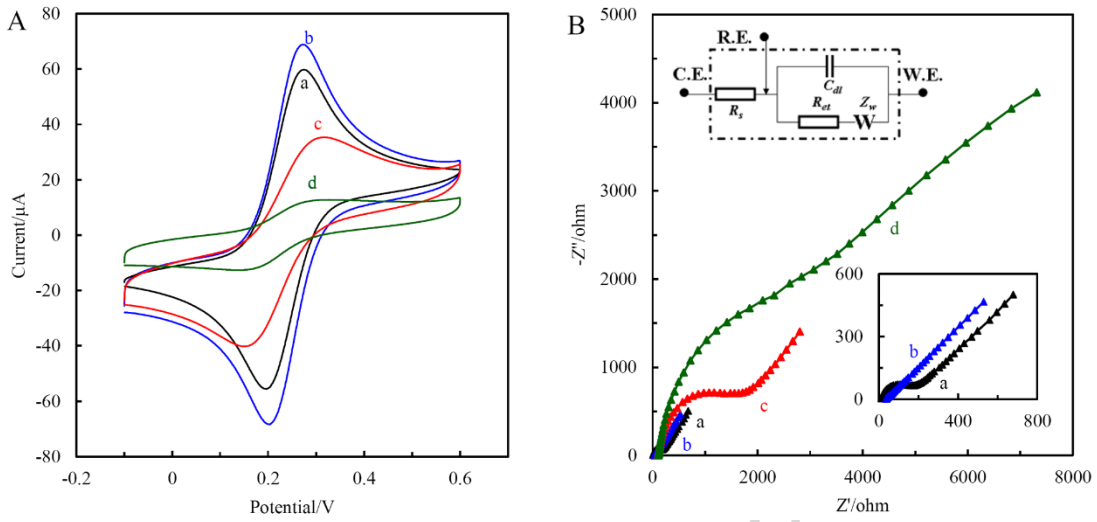

Figure 4 Cyclic voltammograms (A) and electrochemical impedance spectra (B) of GCE (curve a), ERGO-PLL/GCE (curve b), GOx/ERGO-PLL/GCE (curve c) and Nafion/GOx/ERGO-PLL/GCE (curve d) in 100 mM KCl-10 mM PBS (pH 7.40) containing 2.0 mM $K_3Fe(CN)_6/K_4Fe(CN)_6$ (1:1) at scan rate of 100 mV s^{-1}. Frequency range: 10^5 to 1 Hz; potential: 0.24 V; perturbation signal: 5 mV. The inset shows the Randle equivalent circuit applied to fit the impedance spectroscopy.

3.5. Electrochemical behaviors of GOx modified electrodes

The electron transfer behaviors of GOx modified electrodes were investigated in the N_2-saturated and O_2-saturated 100 mM KCl-10 mM PBS (pH 7.40) by cyclic voltammetry. As shown in Fig. 5 and Table 1, while in N_2-saturated PBS system, comparison of bare GCE (curve a), Nafion/GOx/GCE exhibited no redox peaks (curve b). While Nafion/GOx/PLL/GCE (curve d) presented a pair of small redox peaks with the formal potential (E^{Θ}) of -0.444 V, the ΔE_p of 39 mV and the i_{pa}/i_{pc} is 0.57, compared with PLL/GCE (curve c). Moreover, comparison of ERGO/GCE (curve e), Nafion/GOx/ERGO/GCE (curve f) also presented a pair of small redox peaks with the E^{Θ} of -0.474 V, the ΔE_p of 41 mV and the i_{pa}/i_{pc} is 0.70. These results indicate that a weak and quasi-reversible electron transfer between immobilized GOx and PLL nanoparticles modified GCE was presented, as well as that between immobilized GOx and ERGO modified GCE. While Nafion/GOx/ERGO-PLL/GCE (curve h) presented a pair of impressive and well-defined redox peaks with the E^{Θ} of -0.461 V, the ΔE_p of 30 mV and the i_{pa}/i_{pc} is 0.97, compared with ERGO-PLL/GCE

(curve g). Furthermore, the values of redox peak currents were significantly raised 4.3 times for i_{pa} and 2.5 times for i_{pc} as against Nafion/GOx/PLL/GCE, and 2.1 times for i_{pa} and 1.5 times for i_{pc} as against Nafion/GOx/ERGO/GCE, respectively. These results demonstrate that ERGO-PLL hybrid composite film exhibited a distinctly reversible electron transfer between GOx and modified GCE, suggesting that the prepared hybrid nanocomposite was an appropriate media for GOx immobilization and direct electron transfer. The superior electrochemical performance of the ERGO-PLL hybrid composite film modified electrode could be attributed to the fact that there were significant edge-plane-like defective sites, larger surface area, good electronic conductivity, as well as the synergistic effects between ERGO and PLL [23].

While in O_2-saturated PBS system, comparison of bare GCE (curve a′), the reduction peak potential of dissolved oxygen was negatively shifted from -0.31 V to -0.72 V at Nafion/GOx/GCE (curve b′). For the absence of GOx modified electrodes, an obvious reduction peak of dissolved oxygen appeared at -0.28 V for PLL/GCE (curve c′), -0.27 V for ERGO/GCE (curve e′) and -0.29 V for ERGO-PLL/GCE (curve g′), respectively. For the presence of GOx modified electrodes, the reduction peak of dissolved oxygen were negatively shifted to -0.62 V for Nafion/GOx/PLL/GCE (curve d′), -0.63 V for Nafion/GOx/ERGO/GCE (curve f′) and -0.61 V for Nafion/GOx/ERGO-PLL/GCE (curve, h′), respectively. In addition, a weak redox peaks appeared which was direct electron transfer of immobilized GOx with E_{pa} of -0.53 V and E_{pc} of -0.62 V for Nafion/GOx/PLL/GCE (curve d′), E_{pa} of -0.57 V and E_{pc} of -0.63 V for Nafion/GOx/ERGO/GCE (curve f′), E_{pa} of -0.59 V and E_{pc} of -0.61 V for Nafion/GOx/ERGO-PLL/GCE (curve, h′), respectively. These results indicate that the dissolved oxygen has an important effect on direct electron

transfer of GOx.

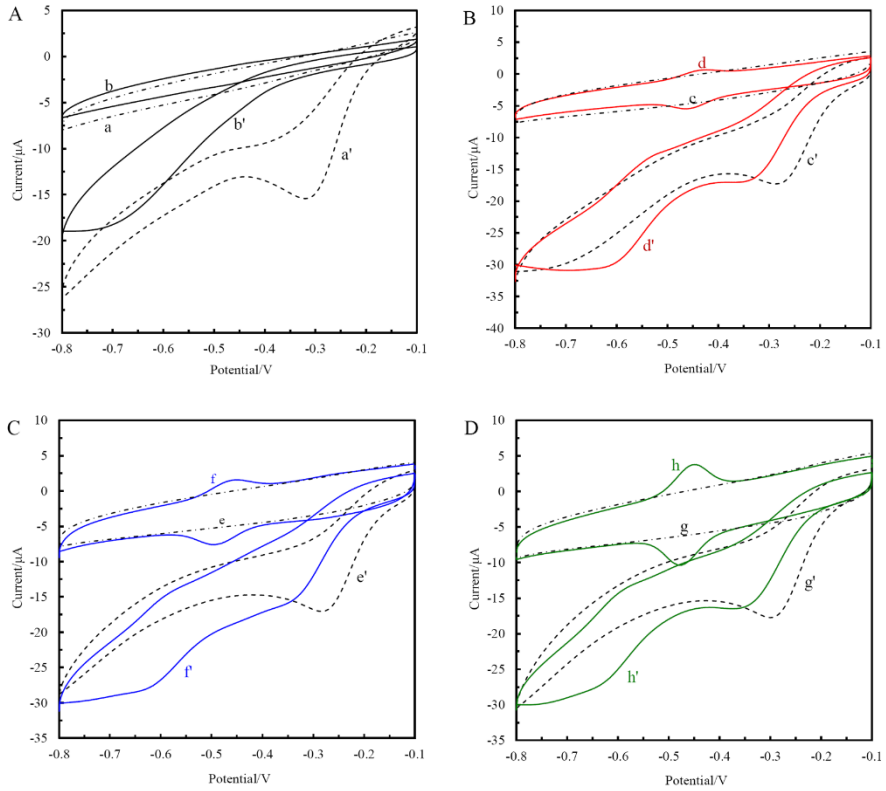

Figure 5 Cyclic voltammograms obtained of (A): GCE (curves a and a′) and Nafion/GOx/GCE (curves b and b′), (B): PLL/GCE (curves c and c′) and Nafion/GOx/PLL/GCE (curves d and d′), (C): ERGO/GCE (curves e and e′) and Nafion/GOx/ERGO/GCE (curves f and f′), (D): ERGO-PLL/GCE (curves g and g′) and Nafion/GOx/ERGO-PLL/GCE (curves h and h′) in N_2-saturated (curves a, b, c, d, e, f, g and h) O_2-saturated (curves a′, b′, c′, d′, e′, f′, g′ and h′) 100 mM KCl-10 mM PBS (pH 7.40) at scan rate of 50 mV s^{-1}.

Table 1. Electrochemical behaviors of GOx modified electrodes in N_2-saturated 100 mM KCl-10 mM PBS (pH 7.40).

Electrodes	E_{pa} (V)	E_{pc} (V)	E^{Θ} (V)	ΔE (mV)	i_{pa} (μA)	i_{pc} (μA)	i_{pa}/i_{pc}
Nafion/GOx/GCE	/	/		/	/	/	/
Nafion/GOx/PLL/GCE	-0.424	-0.463	-0.444	39	0.8	1.4	0.57
Nafion/GOx/ERGO/GCE	-0.454	-0.495	-0.474	41	1.6	2.3	0.70
Nafion/GOx/ERGO-PLL/GCE	-0.446	-0.476	-0.461	30	3.4	3.5	0.97

Fig. 6 displays the cyclic voltammograms of Nafion/GOx/ERGO-PLL/GCE in 10 mM PBS (pH 7.40) at the scan rate from 25 to 1000 mV s^{-1}. It can be seen that the absolute values of redox peak currents linearly increase with the scan rates (Fig. 6B lines, a and b), and a slight shift in redox peak potential is observed (Fig. 6B lines, c

and d). These results indicate that the direct electron transfer process between GOx and modified GCE is surface-confined with a fast electron transfer [29].

The surface coverage (Γ) of electroactive GOx on the modified electrode was calculated as Sharp et al reported method [30]. The Γ obtained was about 1.64×10^{-11} mol cm^{-2} and it was close to that the theoretical value reported for monolayer coverage of GOx (1.89×10^{-11} mol cm^{-2}) [31], and also for GOx immobilized on CdS colloid (1.54×10^{-11} mol cm^{-2}) [32] and on gold nanoparticles (9.8×10^{-12} mol cm^{-2}) [33]. Furthermore, the electron transfer rate constant k_s of immobilized GOx in the Nafion/ERGO-PLL film was estimated as 18.7 s^{-1} according to the model of Laviron [34] using the formula $k_s = mnFv/RT$ which is appropriate when the peak-to-peak separation is less than 200 mV; here m is a parameter related to the peak-to-peak separation, F is Faraday's constant, R is the gas constant, T is the temperature, n is the number of electrons transferred, and v is the scan rate. This value was larger than previously reported values for GOx immobilized in the exfoliated graphite nanosheets and Nafion composite film was 12.6 s^{-1} [35], and also for GOx immobilized on ERGO/sodium dodecyl sulfate film was 4.1 s^{-1} [36], ERGO/PLL composite film was 3.3 s^{-1} [21] and graphene-chitosan nanocomposite was 2.8 s^{-1} [37]. This can be probably attributed to that the rapid charge-transfer of graphene was enhanced by decorating PLL, which acts synergistically with graphene to facilitate charge transfer [19, 38]. In addition, it should be noticed that Nafion used here has two functions, one is to prevent the leakage of immobilized GOx, and the other is to promote the electronic transfer of GOx [35]. These results demonstrate again that the Nafion/GOx/ERGO-PLL/GCE modified electrode provides fast electron transfer between the redox center of GOx and the surface of GCE.

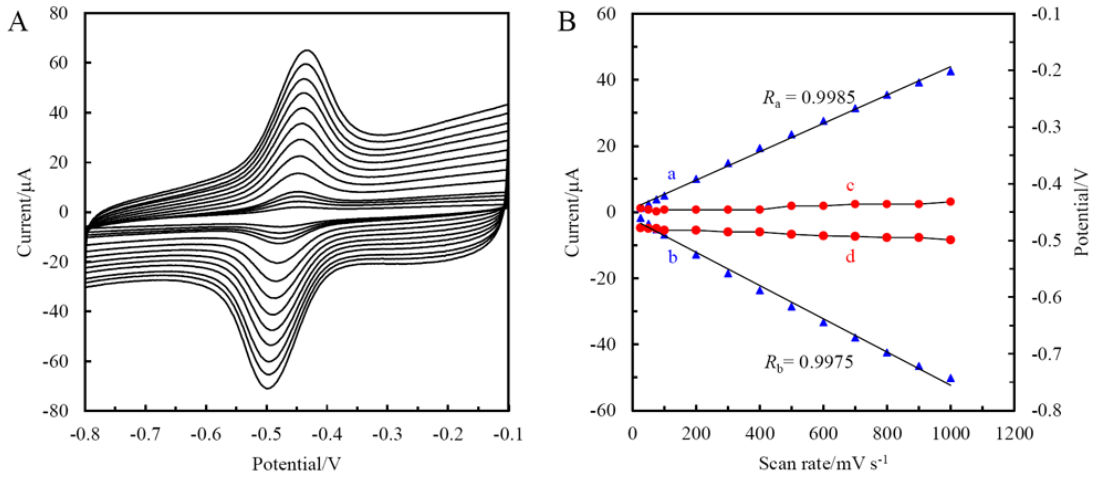

Figure 6 (A) Cyclic voltammograms and (B) the plots of peak currents and potentials of anodic and cathodic versus scan rate obtained of Nafion/GOx/ERGO-PLL/GCE in N_2-saturated 100 mM KCl-10 mM PBS (pH 7.40) at scan rate (from inner to outer), 25, 50, 75, 100, 200, 300, 400, 500, 600, 700, 800, 900 and 1000 mV s^{-1}, lines a and b are the plots of peak currents, and lines c and d are the plots of peak potentials versus scan rate.

From Fig. 7A, it can be seen that the redox peak currents of immobilized GOx increased gradually and then decreased with increasing of pH value, the larger peak currents were obtained at pH 7.4. Therefore, the pH value of supporting electrolyte in following electrochemical measurements was chosen at pH 7.4. Fig. 7B shows that the relationship between the redox peak potentials and the pH value of the solution. It can be seen that the formal potentials E^{Θ} were shifted negatively with the increasing pH value of the solution, suggesting that protons were participated in the electron transfer process of GOx. Furthermore, the linear regression equations of redox peak potentials and pH values can be expressed as E_{pa} (V) = -0.072 - 0.049 pH (R = -0.9894) and E_{pc} (V) = -0.090 - 0.052 pH (R = -0.9920). The slopes obtained are close to the theoretical value of −58.6 mV/pH [39], which indicated that the numbers of electron and proton are equal in the electron transfer process of the immobilized GOx.

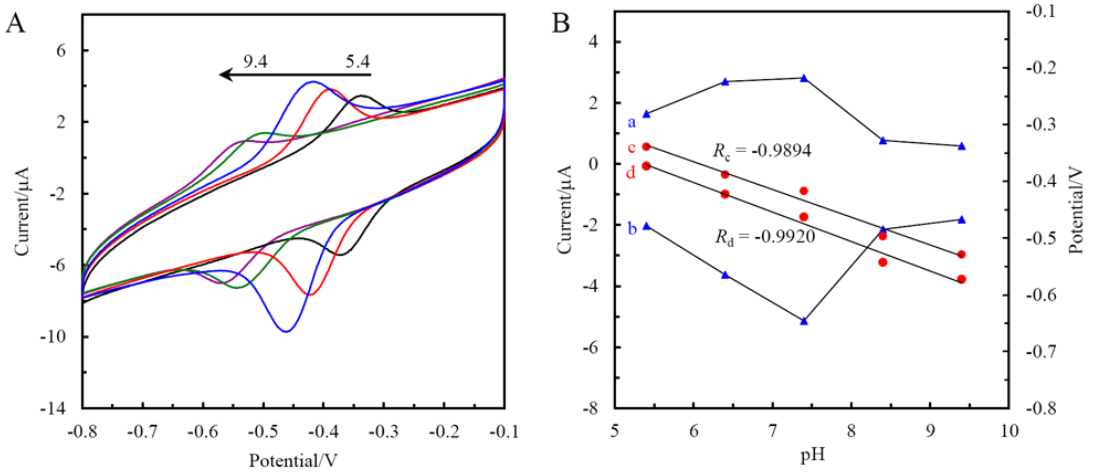

Figure 7 (A) Cyclic voltammograms and (B) effects of pH on the oxidation peak current (line a) and reduction peak current (line b), oxidation peak potential (line c) and reduction peak potential (line d) of Nafion/GOx/ERGO-PLL/GCE in N_2-saturated 100 mM KCl-10 mM PBS with pH values of 5.4, 6.4, 7.4, 8.4 and 9.4 at scan rate of 50 mV s^{-1}.

3.6. Electrocatalytic activities of Nafion/GOx/ERGO-PLL/GCE

The electrocatalytic activities of Nafion/GOx/ERGO-PLL/GCE toward glucose were further investigated by cyclic voltammetry in the absence and presence of oxygen PBS containing different concentrations of glucose (Fig.8). As shown in Fig. 8A, it can be seen that the oxidation peak currents of immobilized GOx were nearly unchanged while the reduction peak currents decreased continuously, and both the oxidation peak potentials and reduction peak potentials were nearly unchanged with increasing glucose concentrations. This result can be attributed to that the direct electron transfer of the immobilized GOx on the Nafion/GOx/ERGO-PLL/GCE in the absence of oxygen PBS is a reversible (the ΔE_p of 30 mV and the i_{pa}/i_{pc} is 0.97) and surface-confined with a fast electron transfer process. The electrode reaction could be expressed as following:

$$GOx\text{-}FAD\ (O) + 2e^- + 2H^+ \leftrightarrow GOx\text{-}FADH_2\ (R) \qquad (1)$$

And when glucose was added to the buffer solution, the enzyme catalysis reaction of immobilized GOx toward glucose comes up on electrode surface:

Glucose + GOx-FAD (O) → Gluconolactone + GOx-$FADH_2$ (R) (2)

In the case of absence of oxygen, the GOx-FAD (O) on the electrode surface was reduced to GOx-$FADH_2$ (R) in two ways. One part was enzyme catalysis reaction and the other part was electrode reaction. However, the total amount of GOx-$FADH_2$ (R) on the electrode surface remain unchanged. Therefore, while continuously added glucose to the buffer solution, the part of enzyme catalysis reaction for GOx-FAD (O) would be increased and that of electrode reaction would be decreased.

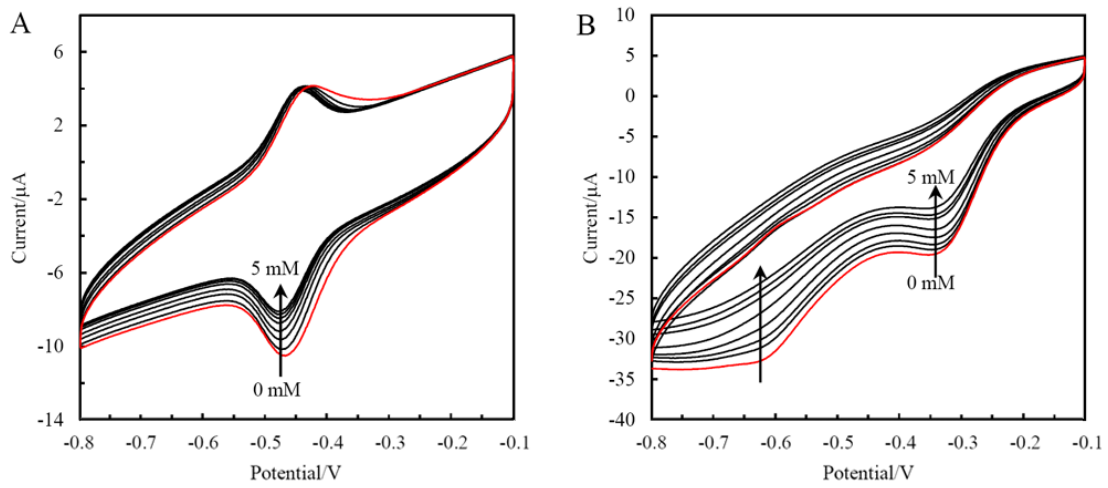

Figure 8 Cyclic voltammograms of Nafion/GOx/ERGO-PLL/GCE in N_2-saturated (A) and O_2-saturated (B) 100 mM KCl-10 mM PBS (pH 7.40) containing different concentrations of glucose (from bottom to top: 0, 0.25, 0.5, 1.0, 2.0, 3.0, 4.0 and 5.0 mM) at scan rate of 50 mV s^{-1}.

As shown in Fig. 8B, it can be seen that two obvious reduction peaks were appeared at about -0.61 V and -0.35 V when Nafion/GOx/ERGO-PLL/GCE in the presence of oxygen PBS containing different concentrations of glucose. And the peak currents of the two reduction peaks decreased continuously while peak potentials are negligibly changed with increasing glucose concentrations. Additionally, the oxidation peaks are very weak and almost invisible, which can be ascribed to that in the presence of oxygen, the reduced enzyme is oxidized quickly at the surface of the

electrode:

$GOx\text{-}FADH_2\ (R) + O_2 \rightarrow GOx\text{-}FAD\ (O) + H_2O_2$ (3)

Therefore, these two reduction peaks of appeared at about -0.61 V and -0.35 V can be ascribed to that the electrochemical reduced processes of oxidation state of GOx-FAD and dissolved oxygen, respectively. For the comparison, the cyclic voltammetric performances of the absence and presence of GOx modified electrodes in the N_2-saturated, air-saturated and O_2-saturated PBS were investigated (as shown in Fig. S1 of supplementary data). The results suggesting that the reduction peak potential of oxidation state of GOx-FAD was negatively shifted from -0.45 V to -0.61 V on Nafion/GOx/ERGO-PLL/GCE in the presence of oxygen PBS, compared with that in the absence of oxygen PBS, and the reduction peak potential of dissolved oxygen was negatively shifted from -0.31 V to -0.35 V in the presence of oxygen PBS on Nafion/GOx/ERGO-PLL/GCE, compared with that on Nafion/ERGO-PLL/GCE. This might due to that the simultaneous presence of oxidation state of GOx-FAD and dissolved oxygen competing and inhibiting each other for their reduction reactions on the modified electrode surface. Furthermore, in the case of presence of oxygen, it is clearly seen that both the reduction peak current of oxygen (at about -0.35 V) and the reduction peak current of oxidation state of GOx-FAD (at about -0.61 V) decreased with increasing glucose concentration, suggesting the consumption of oxygen and the course of the enzyme catalysis reaction of GOx with glucose. However, the reduction peak currents of dissolved oxygen did not change with the addition of glucose on Nafion/ERGO-PLL/GCE (absence of GOx), indicating that the immobilized GOx

showed DET properties have catalytic activity towards glucose oxidation. These results indicated that the immobilized GOx molecules have DET ability are responsible for the glucose oxidation and O_2 consumption.

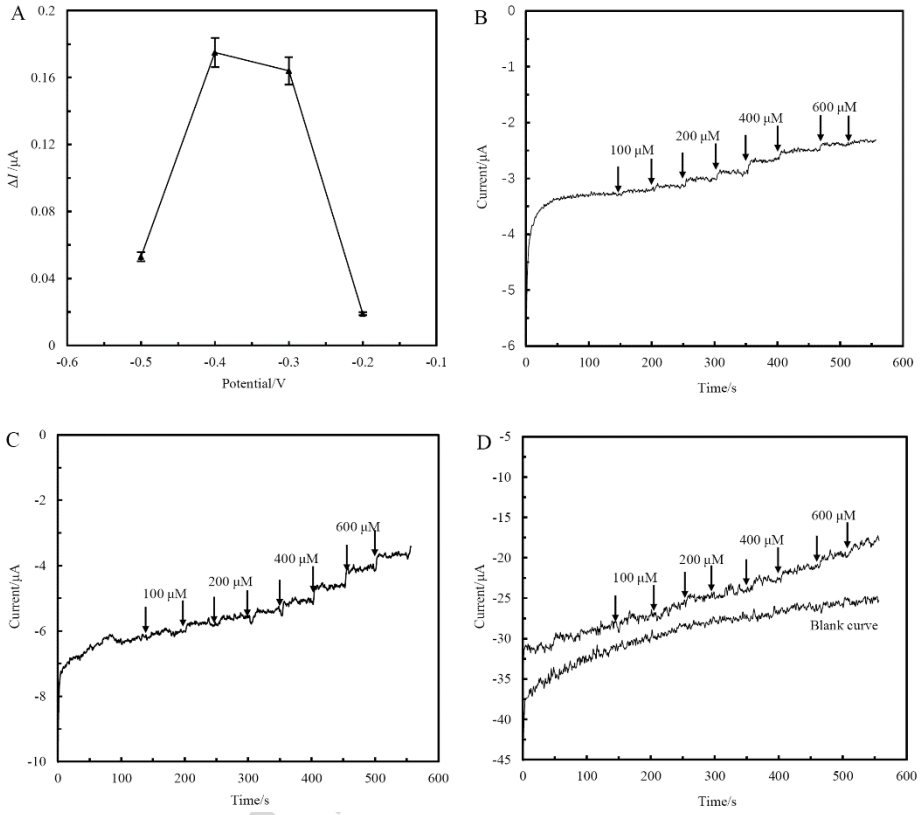

Figure 9 (A) Effects of the applied potential at Nafion/GOx/ERGO-PLL/GCE on the changed of amperometric current (ΔI) for 0.2 mM glucose under N_2-saturated atmosphere. Amperometric response of Nafion/GOx/ERGO-PLL/GCE to the successive injection of glucose into the stirred 100 mM KCl-10 mM PBS (pH 7.40) under (B) N_2-saturated, (C) air-saturated and (D) O_2-saturated atmosphere on -0.4 V.

In order to further approve that the charge transfer process without formation of H_2O_2, we performed two experiments. Firstly, the effects of the applied potential at Nafion/GOx/ERGO-PLL/GCE on the changed of amperometric current (ΔI) for glucose under N_2-saturated atmosphere was investigated. And then the amperometric measurements at the optimized constant potential in the N_2-saturated, air-saturated and O_2-saturated PBS solution for different glucose concentrations were performed,

respectively. From Fig. 9A, it can be seen that the preferable applied potential of the glucose biosensor was -0.4 V. Comparison of the Fig. 9B, C and D, it can be seen that the background current was smaller (~3.5 μA) and went to equilibrium quickly (~100 s) in the N_2-saturated PBS solution (Fig. 9B). Additionally, the amperometric response gradually decreased for the increasing glucose concentration. While in the air-saturated test system, the background current was larger (~6 μA) and went to equilibrium sluggish, and the amperometric response clearly decreased for the increasing glucose concentration (Fig. 9C). In the case of the O_2-saturated PBS solution (Fig. 9D), the background current was the largest (~30 μA) and almost could not went to equilibrium within test time. The results indicating that the consumption of O_2 during the course of amperometric measurement at the applied potential of -0.4 V, which are in accord with the cyclic voltammetric measurements (Fig. 8 and Fig. S1). Furthermore, compared with blank measurement curve in the O_2-saturated PBS system, the amperometric response was nondescript from the background current for the increasing glucose concentration, suggesting that the consumption of O_2 during enzymatic reaction for the case of O_2-saturated is negligible compared to the oxygen level of background and consequently cannot be used to monitor the concentration change of glucose.

Secondly, the cyclic voltammetric and amperometric measurements in the N_2-saturated atmosphere PBS solution for different H_2O_2 concentrations were performed, respectively. From Fig. 10A, it can be seen that the reduction peak currents increased while the oxidation peak currents decreased with the increasing

H_2O_2 concentration, which can be regarded as the increasing of the concentration of oxygen in the test system. This result suggests that the reduction peak currents should be decreased as well as the oxidation peak currents should be increased while the consumption of oxygen in the test system, which is obviously different from that the electrocatalytic activity of glucose (Fig. 8A). From Fig. 10B, it can be seen that the amperometric response also increased clearly with the increasing H_2O_2 concentration, running counter to what the glucose response (Fig. 9B).

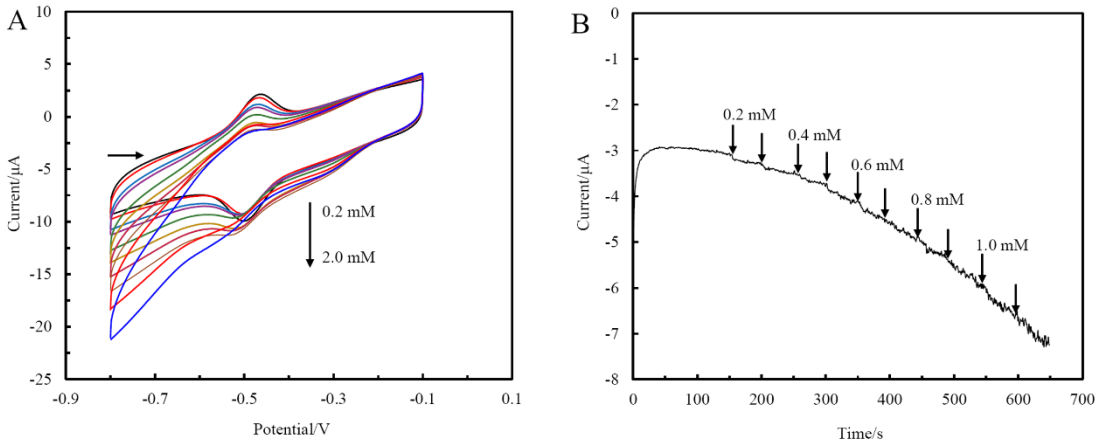

Figure 10 (A) Cyclic voltammograms obtained on Nafion/GOx/ERGO-PLL/GCE in 100 mM KCl-10 mM PBS (pH 7.40) containing 0, 0.2, 0.4, 0.6, 0.8, 1.0, 1.2, 1.6 and 2.0 mM H_2O_2 under N_2-saturated atmosphere at scan rate of 50 mV s^{-1}. (B) Amperometric response of Nafion/GOx/ERGO-PLL/GCE to the successive injection of H_2O_2 into the stirred 100 mM KCl-10 mM PBS (pH 7.40) under N_2-saturated atmosphere on -0.4 V.

From the above, we can demonstrate that the charge transfer of immobilized GOx at the proposed glucose biosensor is O_2-free and without formation of H_2O_2. Direct electron transfer mechanism of immobilized GOx in the Nafion/GOx/ERGO-PLL/GCE was different from that of on the polyphenanthroline modified GCE [40] and hole transporting polymeric semiconductors [41]. There are two types of GOx biosensors, one is real type of third generation biosensor in which GOx-$FADH_2$ transfers electron to the electrode [42]. The other pseudo third

generation type in which the consumption of O_2 is monitored, and GOx has no electrocatalytic effect during the course of enzymatic reaction [43]. In this work, based on the DET of immoblized GOx, the decrease of the reduction current can be used to determination of glucose, the scheme of direct electron transfer of the Nafion/GOx/ERGO-PLL/GCE and the electrocatalysis of glucose and oxygen are shown in Scheme 1.

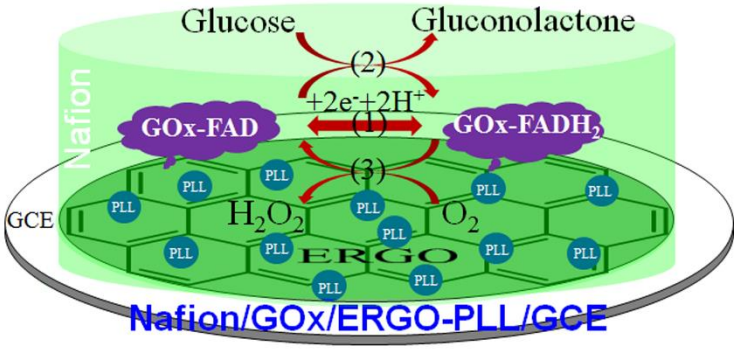

Scheme 1 Schematic illustration of direct electron transfer of the Nafion/GOx/ERGO-PLL/GCE (1), the electrocatalysis of glucose (2) and oxygen (3).

3.7. Determination of glucose

Cyclic voltammetry, differential pulse voltammetry, chronoamperometry and square wave voltammetry (SWV) were performed at the Nafion/GOx/ERGO-PLL/GCE for determination of glucose in the absence and presence of oxygen PBS. It shows that higher current sensitivity and better resolution can be obtained using SWV in the absence of oxygen PBS test system. The SWV profiles obtained for tested different concentrations of glucose besides the plotted calibration curve are shown in Fig. 11. The calibration range of glucose concentration from 0.005 to 10.0 mM. And the statistical analysis of cathodic peak current (I_{ca}) versus the concentrations of glucose revealed three linear ranges (Fig. 11B). The I_{ca} decrease linearly with the increase of the glucose concentration from 0.005 to 0.05

mM, and the linear equation was calibrated as I_a (μA) = 182.2 $C_{glucose}$ (mM) - 30.1 with the correlation coefficient of 0.9915. And the I_{ca} decrease linearly with the increase of the glucose concentration from 0.1 to 1.0 mM, the linear equation was I_b (μA) = 9.1 $C_{glucose}$ (mM) - 19.9 with the correlation coefficient of 0.9850. As well as the I_{ca} decrease linearly with the increase of the glucose concentration from 1.0 to 9.0 mM, the linear equation was I_c (μA) = 0.6 $C_{glucose}$ (mM) - 11.5 with the correlation coefficient of 0.9904. And the sensitivity of the biosensor for glucose detection were about 2579 μA mM^{-1} cm^{-2}, 129 μA mM^{-1} cm^{-2} and 8 μA mM^{-1} cm^{-2} in the concentration range from 0.005 to 0.05 mM, from 0.1 to 1.0 mM and from 1.0 to 9.0 mM, respectivity. The detection limit (defined as 3σ, where σ is the standard deviation of the blank) for glucose was 2.0 μM, and much higher sensitivity 2578.9 μA $mM^{-1}cm^{-2}$ as compared with other nanostructured supports. These performances are improved and comparable with those reported glucose biosensors (Table 2). It is well known that glucose concentration of the diabetic is above 7.0 mM [51], suggesting the proposed biosensor is appropriate for blood sugar monitoring.

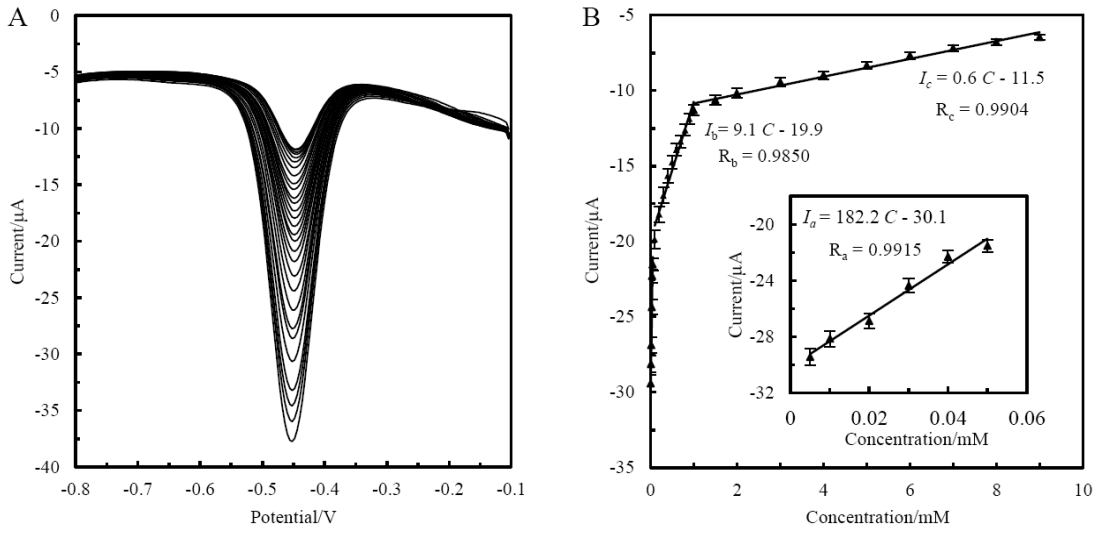

Figure 11 (A) Square wave voltammograms and (B) the reduction peak currents at Nafion/GOx/ERGO-PLL/GCE in N_2-saturated 100 mM KCl-10 mM PBS (pH 7.40) containing different concentrations of glucose (from bottom to top: 0, 0.005, 0.01, 0.02, 0.03, 0.04, 0.05, 0.1, 0.2, 0.3, 0.4, 0.5, 0.6, 0.7, 0.8, 0.9, 1.0, 1.5, 2.0, 3.0, 4.0, 5.0, 6.0, 7.0, 8.0, 9.0, 10.0 mM). Other

condition: 25 mV, 15 Hz and 2.0 s were chosen for amplitude, frequency and quiet time, respectively.

Table 2. Comparison of the performance of glucose biosensors.

Electrode modified materials	Linear range (mM)	Limit of detection (μM)	Sensitivity (μA mM^{-1} cm^{-2})	Reference
Graphene-chitosan	0.08-12.0	20	37.93	[44]
RGO-Fe_3O_4 nanoparticles	0.05-1.0	0.1	5.9	[45]
GO-didodecyldimethylammonium bromide	up to 0.6	20	3.1	[46]
Biomass-derived macroporous carbon	0.007-23.7	2.3	19.16	[47]
RGO-chitosan/concanavalin A	1.0-10.0	-	-	[48]
Nitrogen-doped carbon nanotubes	0.0058-18.0	1.9	29.4	[49]
AuNPs- chitosan /graphene tape electrode	0.616-14.0	202	9	[50]
ERGO-PLL	0.005-0.05 0.1-1.0 1.0-9.0	2.0	2579 129 8	This work

4. Conclusion

In summary, a convenient and simple method of fabricating glucose biosensor is proposed. GOx can be effectively immobilized on ERGO-PLL hybrid composite film which was constructed onto GCE through one step electrodeposition of reduced graphene oxide incorporating polymerized L-lysine from graphene oxide-L-lysine aqueous dispersion. Biocompatible film of Nafion was used here to prevent the leakage of immobilized GOx and meanwhile to promote the electronic transfer of GOx. The fast and direct electron transfer between immobilized GOx with ERGO-PLL and GCE was achieved and the fabricated enzyme biosensor exhibited excellent electrocatalytic activity for the determination of glucose under mediator-free

physiological conditions. This work indicates that the excellent performance of ERGO-PLL hybrid composite film based modified electrode proposed here is superior to that of graphene based, should applied in biosensors, bioelectronics and electrocatalysis etc.

ACKNOWLEDGEMENTS

This work was supported by the National Natural Science Foundation of China (No.21305106) and Shaanxi Province Natural Science Foundation of China (No.2013JQ2013).

References

[1] M. Wooten, S. Karra, M. Zhang, W. Gorski, On the direct electron transfer, sensing, and enzyme activity in the glucose oxidase/carbon nanotubes system, Analytical Chemistry 86, (2014) 752-757.

[2] W. Zhang, G. Li, Third-generation biosensors based on the direct electron transfer of proteins, Analytical Sciences 20, (2004) 603-609.

[3] P. Das, M. Das, S.R. Chinnadayyala, I.M. Singha, P. Goswami, Recent advances on developing 3rd generation enzyme electrode for biosensor applications, Biosensors & Bioelectronics 79, (2016) 386-397.

[4] C. Deng, J. Chen, Z. Nie, S. Si, A sensitive and stable biosensor based on the direct electrochemistry of glucose oxidase assembled layer-by-layer at the multiwall carbon nanotube-modified electrode, Biosensors & Bioelectronics 26, (2010) 213-219.

[5] X. Shangguan, H. Zhang, J. Zheng, Direct electrochemistry of glucose oxidase

based on its direct immobilization on carbon ionic liquid electrode and glucose sensing, Electrochemistry Communications 10, (2008) 1140-1143.

[6] Y. Piao, D.J. Han, T.S. Seo, Highly conductive graphite nanoparticle based enzyme biosensor for electrochemical glucose detection, Sensors and Actuators B: Chemical 194, (2014) 454-459.

[7] C. Shan, H. Yang, J. Song, D. Han, A. Ivaska, L. Niu, Direct electrochemistry of glucose oxidase and biosensing for glucose based on graphene, Analytical Chemistry 81, (2009) 2378-2382.

[8] H. Zhang, Z. Meng, Q. Wang, J. Zheng, A novel glucose biosensor based on direct electrochemistry of glucose oxidase incorporated in biomediated gold nanoparticles–carbon nanotubes composite film, Sensors and Actuators B: Chemical 158, (2011) 23-27.

[9] C. Chen, Q. Xie, D. Yang, H. Xiao, Y. Fu, Y. Tan, S. Yao, Recent advances in electrochemical glucose biosensors: a review, RSC Advances 3, (2013) 4473-4491.

[10] S.K. Vashist, J.H.T. Luong, Recent advances in electrochemical biosensing schemes using graphene and graphene-based nanocomposites, Carbon 84, (2015) 519-550.

[11] S. Guo, S. Dong, Graphene nanosheet: synthesis, molecular engineering, thin film, hybrids, and energy and analytical applications. Chemical Society reviews 40, (2011) 2644-2672.

[12] B. Liang, L. Fang, G. Yang, Y. Hu, X. Guo, X. Ye, Direct electron transfer

glucose biosensor based on glucose oxidase self-assembled on electrochemically reduced carboxyl graphene, Biosensors & Bioelectronics 43, (2013) 131-136.

[13] C. Shan, H. Yang, D. Han, Q. Zhang, A. Ivaska, L. Niu, Graphene/AuNPs/chitosan nanocomposites film for glucose biosensing, Biosensors & Bioelectronics 25, (2010) 1070-1074.

[14] X. Feng, H. Cheng, Y. Pan, H. Zheng, Development of glucose biosensors based on nanostructured graphene-conducting polyaniline composite, Biosensors & Bioelectronics 70, (2015) 411-417.

[15] P. Rafighi, M. Tavahodi, B. Haghighi, Fabrication of a third-generation glucose biosensor using graphene-polyethyleneimine-gold nanoparticles hybrid, Sensors and Actuators B: Chemical 232, (2016) 454-461.

[16] Y. Zhao, W. Li, L. Pan, D. Zhai, Y. Wang, L. Li, W. Chen, W. Yin, X. Wang, J.B. Xu, Y. Shi, ZnO-nanorods/graphene heterostructure: a direct electron transfer glucose biosensor, Scientific Reports 6, (2016) 32327.

[17] Q. Ren, L. Feng, R. Fan, X. Ge, Y. Sun, Water-dispersible triethylenetetramine-functionalized graphene: preparation, characterization and application as an amperometric glucose sensor, Materials Science & Engineering C, Materials for Biological Applications 68, (2016) 308-316.

[18] S. Pakapongpan, R.P. Poo-Arporn, Self-assembly of glucose oxidase on reduced graphene oxide-magnetic nanoparticles nanocomposite-based direct electrochemistry for reagentless glucose biosensor, Materials Science & Engineering C, Materials for Biological Applications 76, (2017) 398-405.

[19] W. Sun, Y. Wang, Y. Zhang, X. Ju, G. Li, Z. Sun, Poly(methylene blue) functionalized graphene modified carbon ionic liquid electrode for the electrochemical detection of dopamine, Analytica Chimica Acta 751, (2012) 59-65.

[20] R.d.C.S. Luz, F.S. Damos, A.A. Tanaka, L.T. Kubota, Dissolved oxygen sensor based on cobalt tetrasulphonated phthalocyanine immobilized in poly-l-lysine film onto glassy carbon electrode, Sensors and Actuators B: Chemical 114, (2006) 1019-1027.

[21] L. Hua, X. Wu, R. Wang, Glucose sensor based on an electrochemical reduced graphene oxide-poly(L-lysine) composite film modified GC electrode, The Analyst 137, (2012) 5716-5719.

[22] H. Chen, Y. Cui, B. Zhang, B. Liu, G. Chen, D. Tang, Poly(o-phenylenediamine)-carried nanogold particles as signal tags for sensitive electrochemical immunoassay of prolactin, Analytica Chimica Acta 728, (2012) 18-25.

[23] D. Zhang, L. Li, W. Ma, X. Chen, Y. Zhang Electrodeposited reduced graphene oxide incorporating polymerization of l-lysine on electrode surface and its application in simultaneous electrochemical determination of ascorbic acid, dopamine and uric acid, Materials Science & Engineering C, Materials for Biological Applications 70, (2017) 241-249.

[24] W.S. Hummers, R.E.Offeman, Preparation of graphitic oxide. Journal of the American Chemical Society 80, (1958) 1339.

[25] D. Zhang, L. Fu, L. Liao, B. Dai, R. Zou, C. Zhang, Electrochemically functional graphene nanostructure and layer-by-layer nanocomposite incorporating adsorption of electroactive methylene blue, Electrochimica Acta 75, (2012) 71-79.

[26] D. Zhang, Y. Zhang, L. Zheng, Y. Zhan, L. He, Graphene oxide/poly-L-lysine assembled layer for adhesion and electrochemical impedance detection of leukemia K562 cancer cells, Biosensors & Bioelectronics 42, (2013) 112-118.

[27] J. Bonor, V. Reddy, H. Akkiraju, P. Dhurjati, A. Nohe, Synthesis and characterization of L-Lysine conjugated silver nanoparticles smaller than 10 nM, Advanced Science, Engineering and Medicine 6, (2014) 942-947.

[28] B. Huang, N. Jia, L. Chen, L. Tan, S. Yao Electrochemical impedance spectroscopy study on polymerization of L-lysine on electrode surface and its application for immobilization and detection of suspension cells, Analytical Chemistry 86, (2014) 6940-6947.

[29] A.J. Bard, L.R. Faulkner, Electrochemical methods: fundamentals and applications. New York: Wiley, 2001.

[30] M. Sharp, M. Petersson, K. Edström, Preliminary determinations of electrontransfer kinetics involving ferrocene covalently attached to a platinumsurface, Journal of Electroanalytical Chemistry 95, (1979) 123-130.

[31] S.F. Wang, T. Chen, Z.L. Zhang, X.C. Shen, Z.X. Lu, D.W. Pang, K.Y. Wong, Direct electrochemistry and electrocatalysis of heme proteins entrapped inagarose hydrogel films in room-temperature ionic liquids, Langmuir 21, (2005)

9260-9266.

[32] Y. Huang, W. Zhang, H. Xiao, G. Li, An electrochemical investigation of glucose oxidase at a CdS nanoparticles modified electrode, Biosensors & Bioelectronics 21, (2005) 817-821.

[33] S. Liu, H. Ju, Reagentless glucose biosensor based on direct electron transfer ofglucose oxidase immobilized on colloidal gold modified carbon pasteelectrode, Biosensors & Bioelectronics 19, (2003) 177-183.

[34] E. Laviron, General expression of the linear potential sweep voltammogram in the case of diffusionless electrochemical systems, Journal of Electroanalytical Chemistry 101, (1979) 19-28.

[35] C. Fu, W. Yang, X. Chen, D.G. Evans, Direct electrochemistry of glucose oxidase on a graphite nanosheet–Nafion composite film modified electrode, Electrochemistry Communications 11, (2009) 997-1000.

[36] M. Shamsipur, M.A. Tabrizi, Achieving direct electrochemistry of glucose oxidase by one step electrochemical reduction of graphene oxide and its use in glucose sensing, Materials science & engineering C, Materials for Biological Applications 45, (2014) 103-108.

[37] X. Kang, J. Wang, H. Wu, I.A. Aksay, J. Liu, Y. Lin Glucose oxidase-graphene-chitosan modified electrode for direct electrochemistry and glucose sensing, Biosensors & Bioelectronics 25, (2009) 901-905.

[38] D. Zhang, L. Fu, L. Liao, N. Liu, B. Dai, C. Zhang, Preparation, characterization, and application of electrochemically functional graphene nanocomposites by

one-step liquid-phase exfoliation of natural flake graphite with methylene blue, Nano Research 5, (2012) 875-887.

[39] Q. Liu, X. Lu, J. Li, X. Yao, J. Li, Direct electrochemistry of glucose oxidase and electrochemical biosensing of glucose on quantum dots/carbon nanotubes electrodes, Biosensors & Bioelectronics 22, (2007) 3203-3209.

[40] Y. Oztekin, A. Ramanaviciene, Z. Yazicigil, A.O. Solak, A. Ramanavicius, Direct electron transfer from glucose oxidase immobilized on polyphenanthroline modified-glassy carbon electrode. Biosensors & Bioelectronics 26, (2011) 2541-2546.

[41] G. Bagdžiūnas, Š. Žukauskas, A. Ramanavičius, Insights into hole transfer mechanism between glucose oxidase and p-Type organic semiconductor. Biosensors & Bioelectronics 102, (2018) 449-455.

[42] P. Rafighi, M. Tavahodi, B. Haghighi, Fabrication of a third-generation glucose biosensor using graphene-polyethyleneimine-gold nanoparticles hybrid, Sensors and Actuators B 232, (2016) 454-461.

[43] B. Haghighi, M.A. Tabrizi, Direct electron transfer from glucose oxidase immobilized on a nano-porous glassy carbon electrode, Electrochimica Acta 56, (2011) 10101-10106.

[44] X. Kang, J. Wang, H. Wu, I.A. Aksay, J. Liu, Y. Lin, Glucose oxidase-graphene-chitosan modified electrode for direct electrochemistry and glucose sensing, Biosensors & Bioelectronics 25, (2009) 901-905.

[45] S. Pakapongpan, R.P. Poo-arporn, Self-assembly of glucose oxidase on reduced

graphene oxide-magnetic nanoparticles nanocomposite-based direct electrochemistry for reagentless glucose biosensor, Materials Science and Engineering: C 76 (2017) 398-405.

[46] S. Castrignanò, F. Valetti, G. Gilardi, S.J. Sadeghi, Graphene oxide-mediated electrochemistry of glucose oxidase on glassy carbon electrodes, Biotechnology and Applied Biochemistry 63, (2016) 157-162.

[47] L.Wang, Q. Zhang, S. Chen, F. Xu, S. Chen, J. Jia, H. Tan, H. Hou, Y. Song, Electrochemical sensing and biosensing platform based on biomass-derived macroporous carbon materials, Analytical Chemistry 86, (2014) 1414-1421.

[48] Y. Song, H. Liu, H. Tan, F. Xu, J. Jia, L. Zhang, Z. Li, L. Wang, pH-Switchable electrochemical sensing platform based on chitosan-reduced graphene oxide/concanavalin A layer for assay of glucose and urea, Analytical Chemistry 86, (2014) 1980-1987.

[49] Y. Song, X. Lu, Y. Li, Q. Guo, S. Chen, L. Mao, H. Hou, L. Wang, Nitrogen-doped carbon nanotubes supported by macroporous carbon as an efficient enzymatic biosensing platform for glucose, Analytical Chemistry 88, (2016) 1371-1377.

[50] L. Wang, J. Yu, Y. Zhang, H. Yang, L. Miao, Y. Song, Simple and large-scale strategy to prepare flexible graphene tape electrode, ACS Applied Materials & Interfaces 9, (2017) 9089-9095.

[51] Z.H. Dai, J. Ni, X.H. Huang, G.F. Lu, J.C. Bao, Direct electrochemistry of glucose oxidase immobilized on a hexagonal mesoporous silica-MCM-41 matrix,

Bioelectrochemistry 70, (2007) 250-256.

Figure Captions

Scheme 1 Schematic illustration of direct electron transfer of the Nafion/GOx/ERGO-PLL/GCE (1) and the electrocatalysis of glucose (2) and oxygen (3).

Figure 1 FT-IR spectra of graphene oxide (curve a), L-lysine (curve b) and graphene oxide- L-lysine (curve c).

Figure 2 Cyclic voltammograms obtained of GCE in continuously stirring condition of N_2-saturated 100 mM KCl-10 mM PBS (pH 7.40) containing 1.0 mg mL^{-1} GO and 1.0 mM L-lysine (5:2, v/v) scan from -1.5V to 2.2V for 8 circles with a scan rate of 25 mV/s.

Figure 3 SEM images of PLL/GCE (A), ERGO/GCE (B), ERGO-PLL/GCE (C) and Nafion/GOx/ERGO-PLL/GCE (D).

Figure 4 Cyclic voltammograms (A) and electrochemical impedance spectra (B) of GCE (curve a), ERGO-PLL/GCE (curve b), GOx/ERGO-PLL/GCE (curve c) and Nafion/GOx/ERGO-PLL/GCE (curve d) in 100 mM KCl-10 mM PBS (pH 7.40) containing 2.0 mM $K_3Fe(CN)_6/K_4Fe(CN)_6$ (1:1) at scan rate of 100 mV s^{-1}. Frequency range: 10^5 to 1 Hz; potential: 0.24 V; perturbation signal: 5 mV. The inset

shows the Randle equivalent circuit applied to fit the impedance spectroscopy.

Figure 5 Cyclic voltammograms obtained of (A): GCE (curves a and a′) and Nafion/GOx/GCE (curves b and b′), (B): PLL/GCE (curves c and c′) and Nafion/GOx/PLL/GCE (curves d and d′), (C): ERGO/GCE (curves e and e′) and Nafion/GOx/ERGO/GCE (curves f and f′), (D): ERGO-PLL/GCE (curves g and g′) and Nafion/GOx/ERGO-PLL/GCE (curves h and h′) in N_2-saturated (curves a, b, c, d, e, f, g and h) O_2-saturated (curves a′, b′, c′, d′, e′, f′, g′ and h′) 100 mM KCl-10 mM PBS (pH 7.40) at scan rate of 50 mV s^{-1}.

Figure 6 (A) Cyclic voltammograms and (B) the plots of peak currents and potentials of anodic and cathodic versus scan rate obtained of Nafion/GOx/ERGO-PLL/GCE in N_2-saturated 100 mM KCl-10 mM PBS (pH 7.40) at scan rate (from inner to outer), 25, 50, 75, 100, 200, 300, 400, 500, 600, 700, 800, 900 and 1000 mV s^{-1}, lines a and b are the plots of peak currents, and lines c and d are the plots of peak potentials versus scan rate.

Figure 7 (A) Cyclic voltammograms and (B) effects of pH on the oxidation peak current (line a) and reduction peak current (line b), oxidation peak potential (line c) and reduction peak potential (line d) of Nafion/GOx/ERGO-PLL/GCE in N_2-saturated 100 mM KCl-10 mM PBS with pH values of 5.4, 6.4, 7.4, 8.4 and 9.4 at scan rate of 50 mV s^{-1}.

Figure 8 Cyclic voltammograms of Nafion/GOx/ERGO-PLL/GCE in N_2-saturated (A) and O_2-saturated (B) 100 mM KCl-10 mM PBS (pH 7.40) containing different concentrations of glucose (from bottom to top: 0, 0.25, 0.5, 1.0, 2.0, 3.0, 4.0 and 5.0 mM) at scan rate of 50 mV s^{-1}.

Figure 9 (A) Effects of the applied potential at Nafion/GOx/ERGO-PLL/GCE on the changed of amperometric current (ΔI) for 0.2 mM glucose under N_2-saturated

atmosphere. Amperometric response of Nafion/GOx/ERGO-PLL/GCE to the successive injection of glucose into the stirred 100 mM KCl-10 mM PBS (pH 7.40) under (B) N_2-saturated, (C) air-saturated and (D) O_2-saturated atmosphere on -0.4 V.

Figure 10 (A) Cyclic voltammograms obtained on Nafion/GOx/ERGO-PLL/GCE in 100 mM KCl-10 mM PBS (pH 7.40) containing 0, 0.2, 0.4, 0.6, 0.8, 1.0, 1.2, 1.6 and 2.0 mM H_2O_2 under N_2-saturated atmosphere at scan rate of 50 mV s^{-1}. (B) Amperometric response of Nafion/GOx/ERGO-PLL/GCE to the successive injection of H_2O_2 into the stirred 100 mM KCl-10 mM PBS (pH 7.40) under N_2-saturated atmosphere on -0.4 V.

Figure 11 (A) Square wave voltammograms and (B) the reduction peak currents at Nafion/GOx/ERGO-PLL/GCE in N_2-saturated 100 mM KCl-10 mM PBS (pH 7.40) containing different concentrations of glucose (from bottom to top: 0, 0.005, 0.01, 0.02, 0.03, 0.04, 0.05, 0.1, 0.2, 0.3, 0.4, 0.5, 0.6, 0.7, 0.8, 0.9, 1.0, 1.5, 2.0, 3.0, 4.0, 5.0, 6.0, 7.0, 8.0, 9.0, 10.0 mM). Other condition: 25 mV, 15 Hz and 2.0 s were chosen for amplitude, frequency and quiet time, respectively.

Highlights

- A convenient and simple method of fabricating glucose biosensor is proposed.
- Graphene hybrid composite ERGO-PLL was prepared by one step electrodeposition technology.
- The fast and direct electron transfer between immobilized GOx with ERGO-PLL and GCE was achieved.

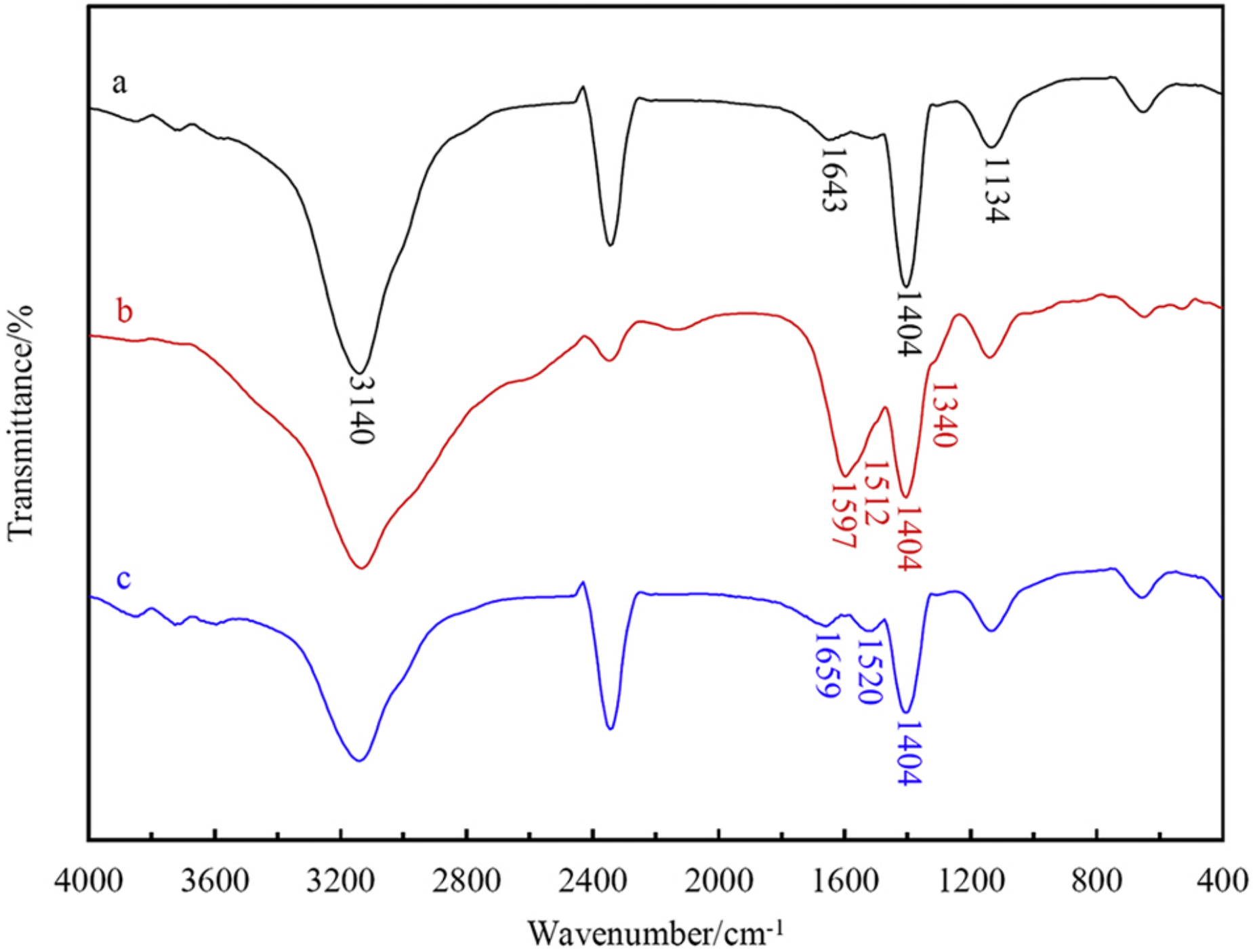
a
b
c
3140
1643
1404
1134
1597
1512
1404
1340
1659
1520
1404
Transmittance/%
4000
3600
3200
2800
2400
2000
1600
1200
800
400
Wavenumber/cm-1

Figure 1

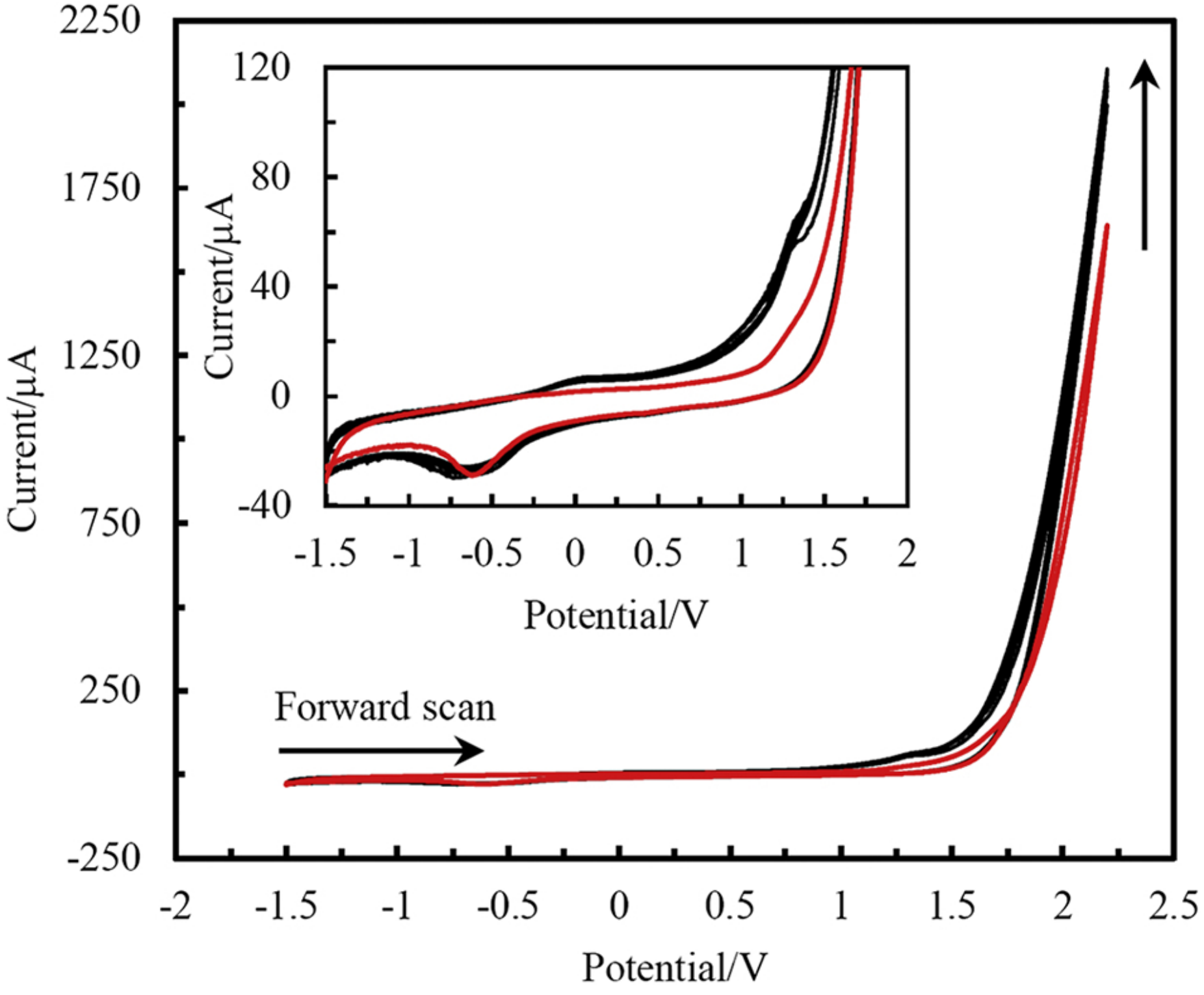
2250
1750
1250
750
250
-250
Current/μA
-2
-1.5
-1
-0.5
0
0.5
1
1.5
2
2.5
Potential/V
Forward scan
120
80
40
0
-40
Current/μA
-1.5
-1
-0.5
0
0.5
1
1.5
2
Potential/V

Figure 2

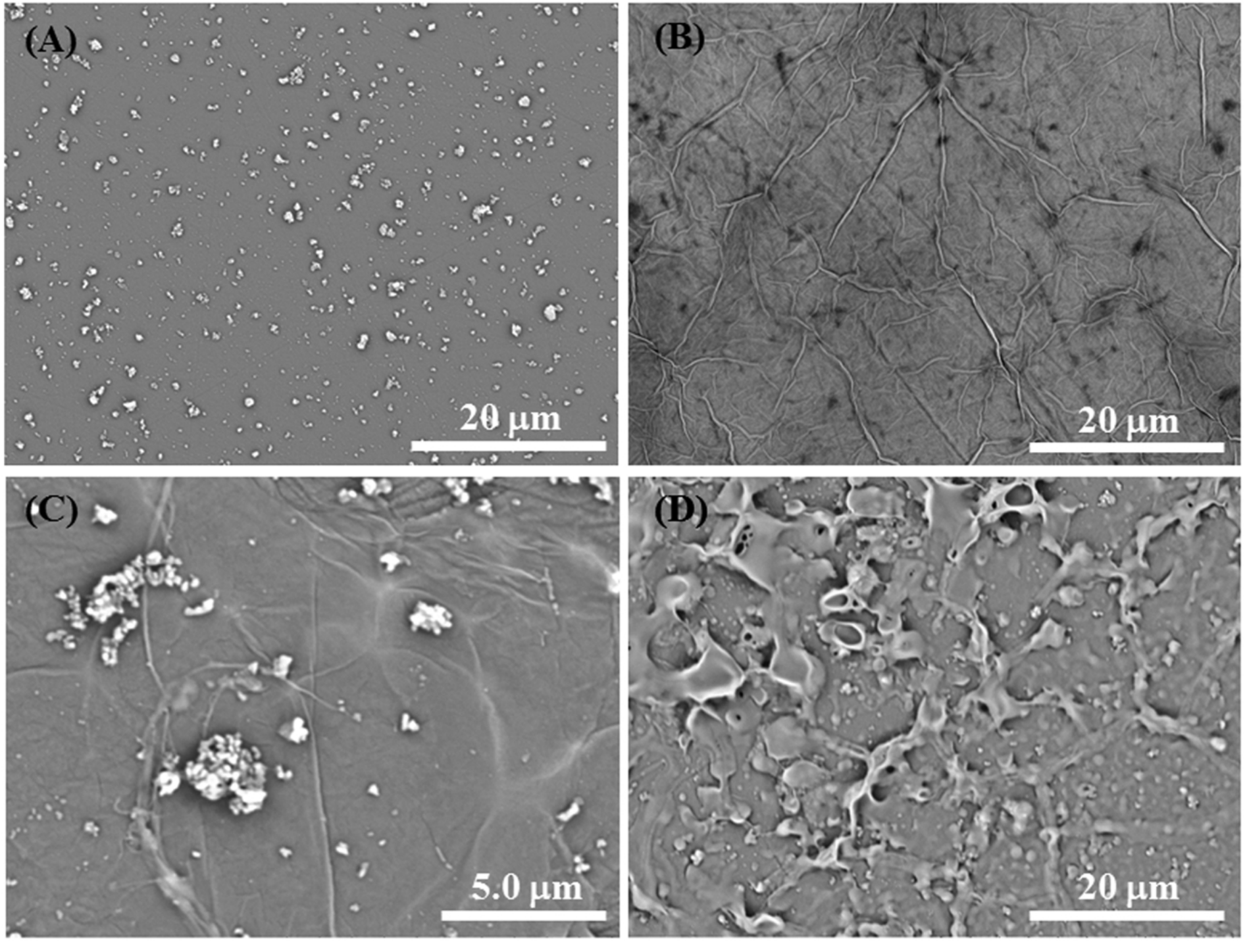

Figure 3

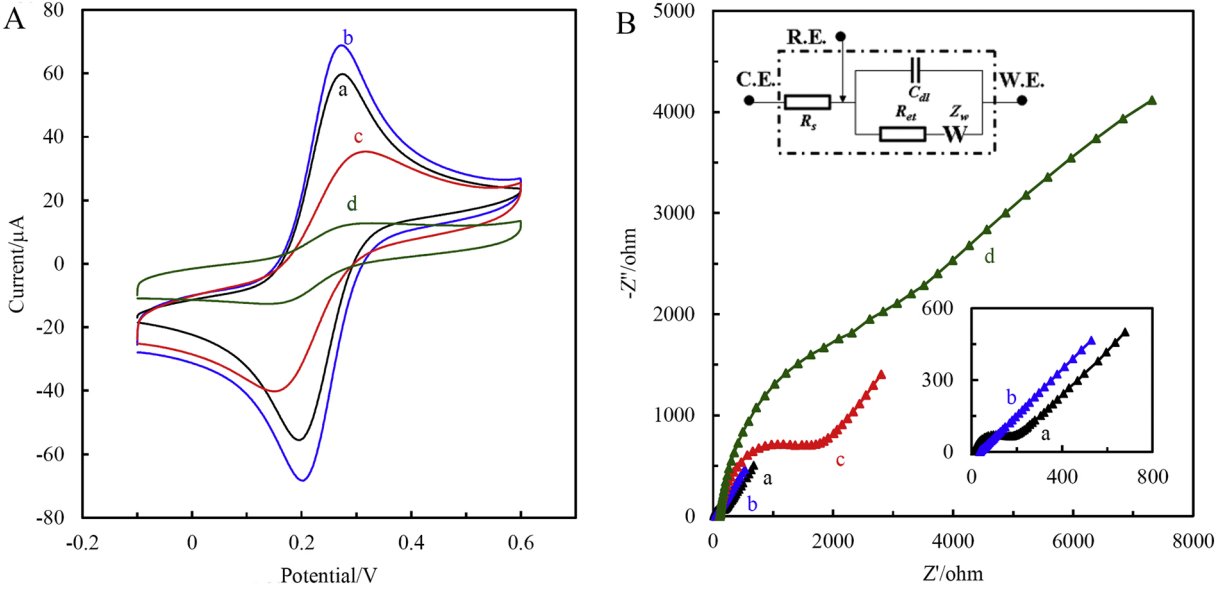
A
Current/μA
Potential/V
a
b
c
d
B
-Z''/ohm
Z'/ohm
R.E.
C.E.
W.E.
C_{dl}
R_s
R_{et}
Z_w
W

Figure 4

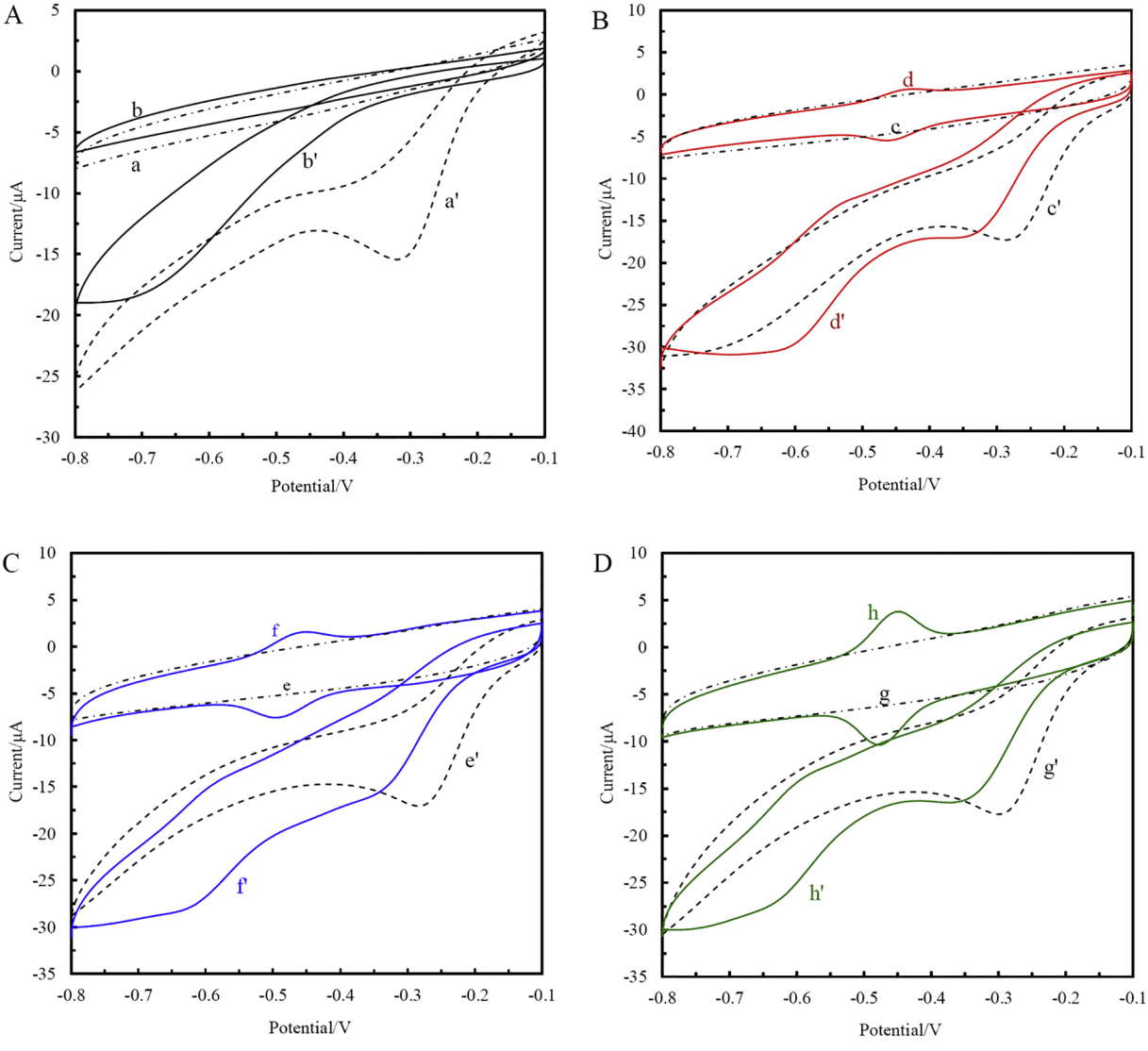

Figure 5

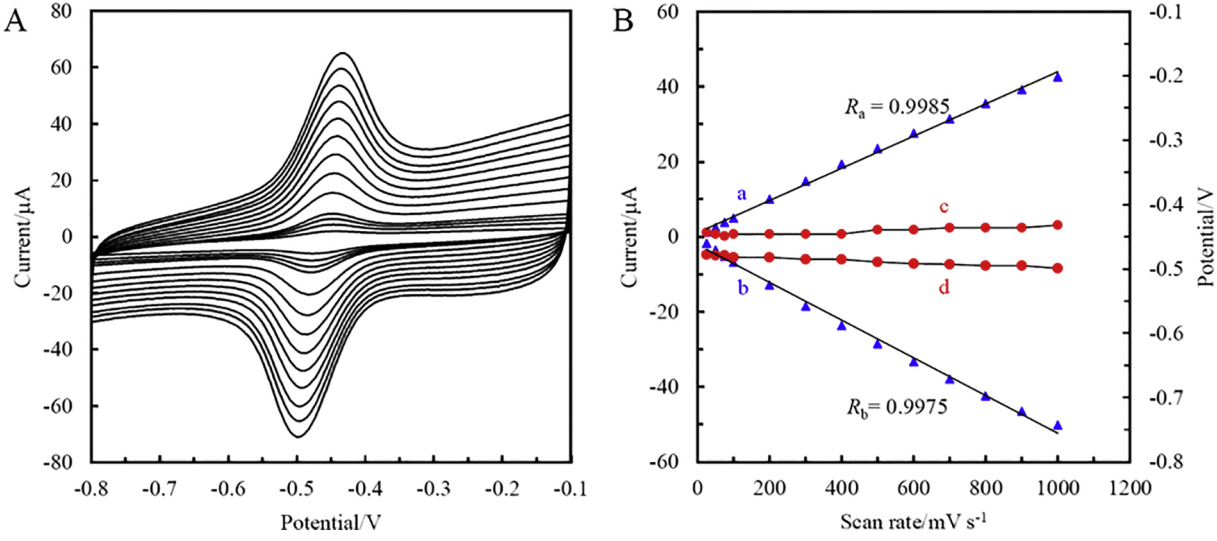
A
Current/μA
Potential/V
B
Current/μA
Potential/V
Scan rate/mV s-1
Ra = 0.9985
Rb= 0.9975
a
b
c
d

Figure 6

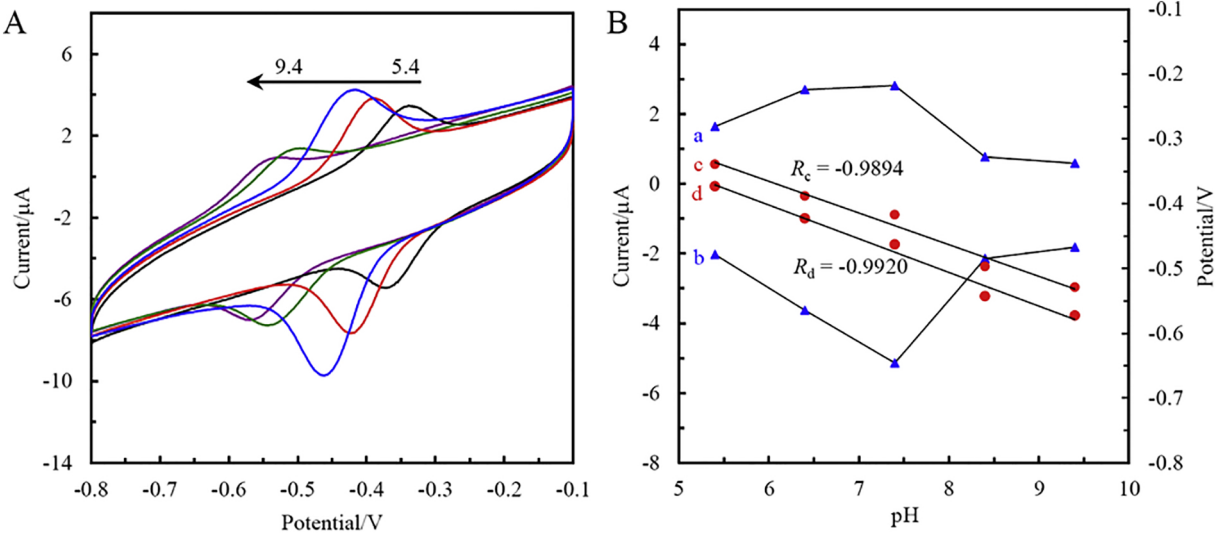
A
9.4
5.4
Current/μA
Potential/V
B
a
c
d
b
R_c = -0.9894
R_d = -0.9920
Current/μA
Potential/V
pH

Figure 7

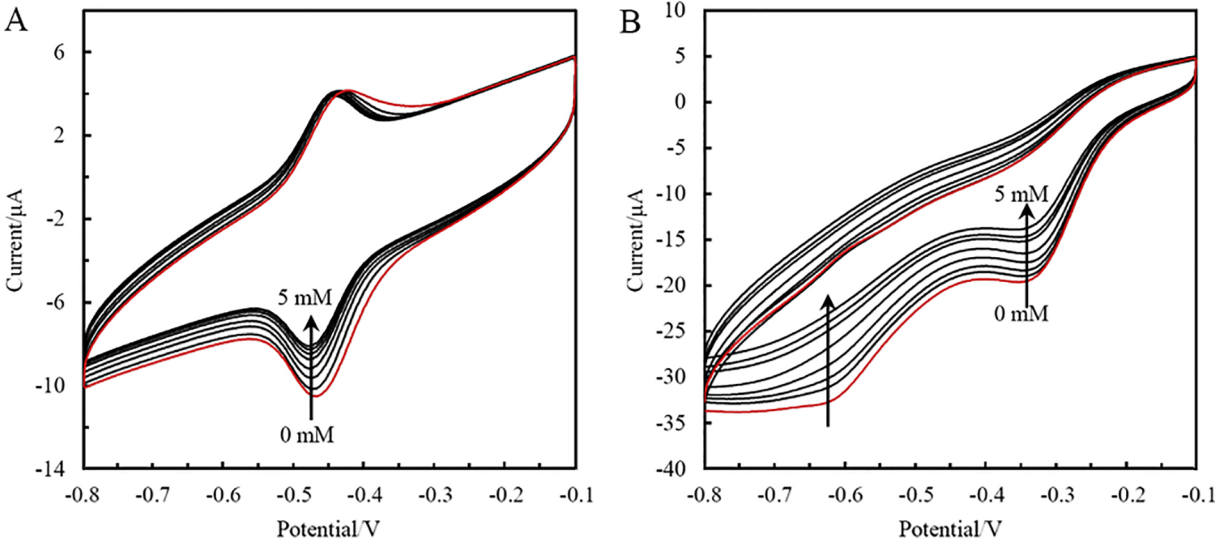
A
6
2
-2
-6
-10
-14
Current/μA
5 mM
0 mM
-0.8
-0.7
-0.6
-0.5
-0.4
-0.3
-0.2
-0.1
Potential/V
B
10
5
0
-5
-10
-15
-20
-25
-30
-35
-40
Current/μA
5 mM
0 mM
-0.8
-0.7
-0.6
-0.5
-0.4
-0.3
-0.2
-0.1
Potential/V

Figure 8

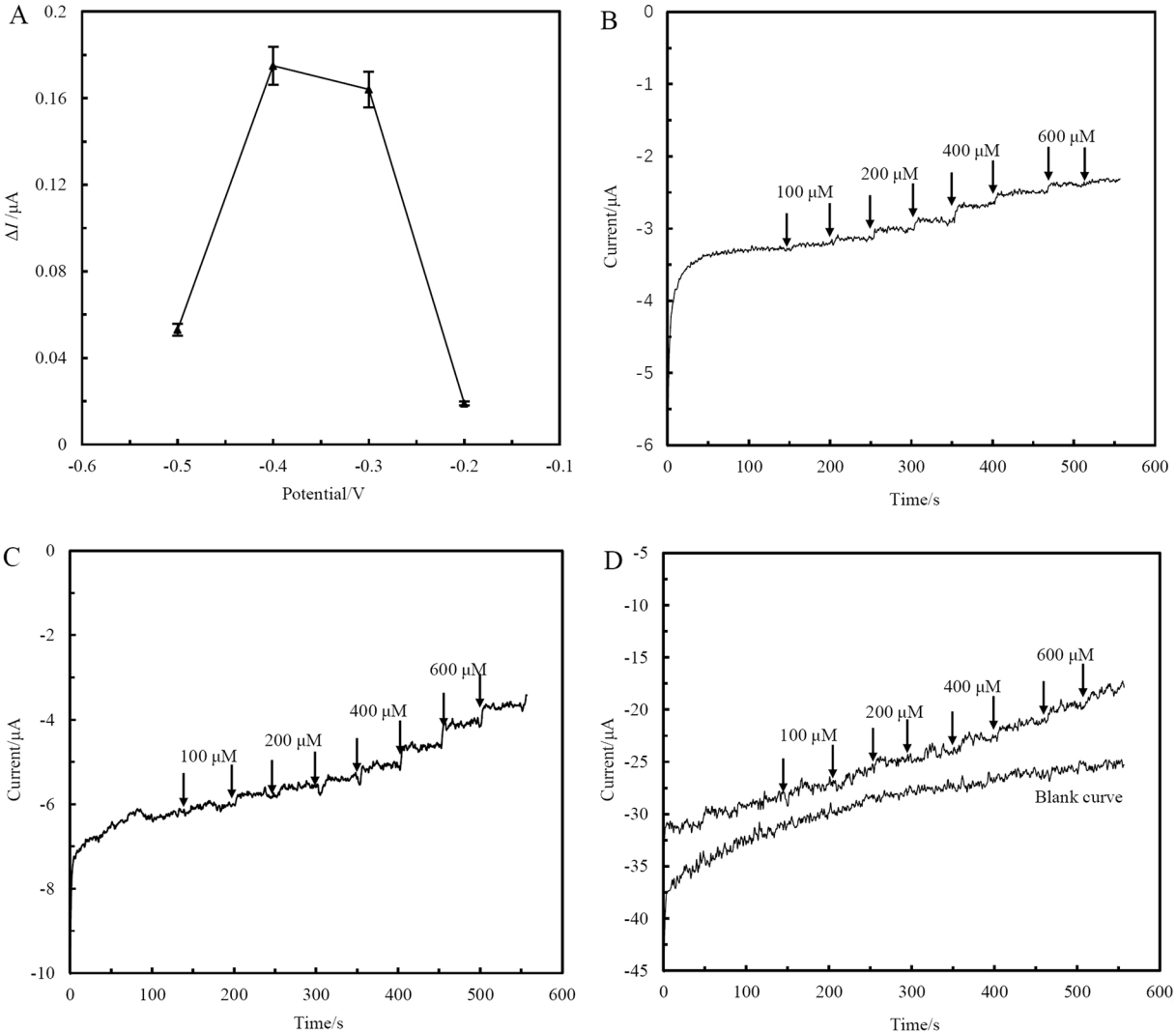
A
ΔI /μA
Potential/V
B
Current/μA
Time/s
100 μM
200 μM
400 μM
600 μM
C
Current/μA
Time/s
100 μM
200 μM
400 μM
600 μM
D
Current/μA
Time/s
100 μM
200 μM
400 μM
600 μM
Blank curve

Figure 9

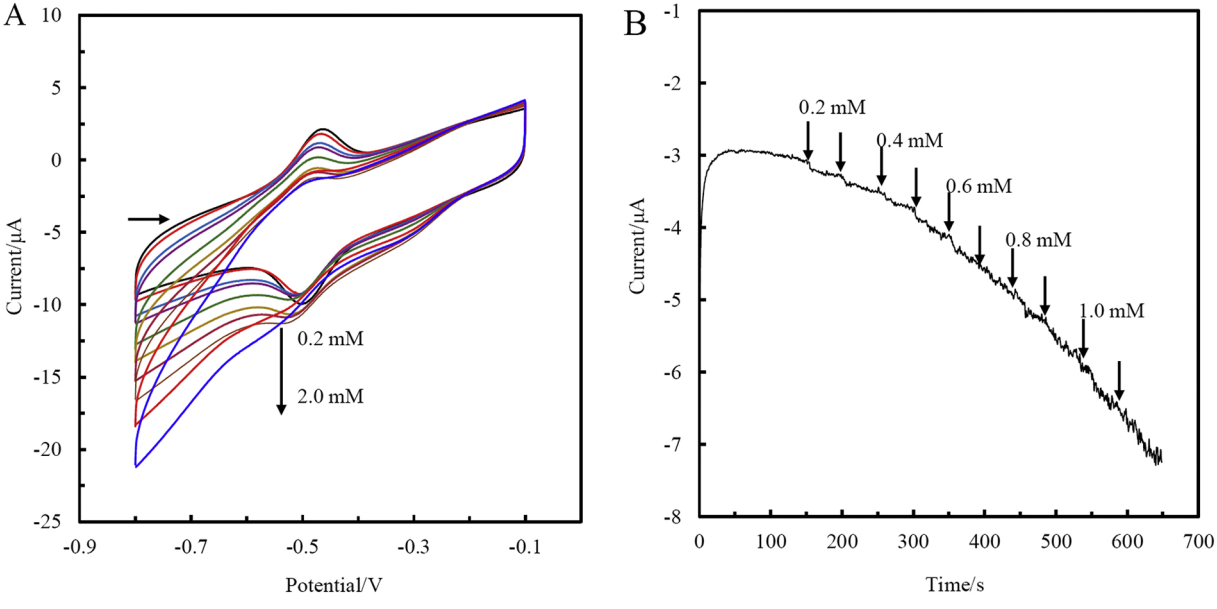
A
Current/μA
Potential/V
0.2 mM
2.0 mM
B
Current/μA
Time/s
0.2 mM
0.4 mM
0.6 mM
0.8 mM
1.0 mM

Figure 10

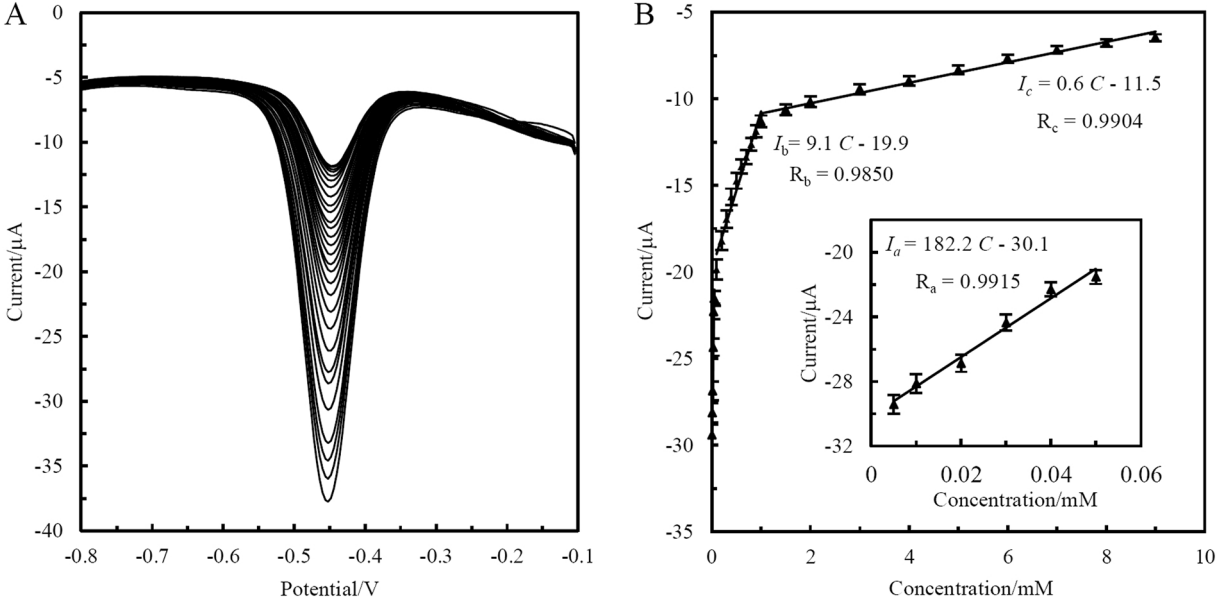
A
Current/μA
Potential/V
B
Current/μA
Concentration/mM
I_c = 0.6 C - 11.5
R_c = 0.9904
I_b= 9.1 C - 19.9
R_b = 0.9850
I_a = 182.2 C - 30.1
R_a = 0.9915
Current/μA
Concentration/mM

Figure 11